2011

Surface Functionalization of Polymer Vesicles with Dendritic Groups: Effects on Physical and Biological Properties

Ryan C. Amos

Surface Functionalization of Polymer Vesicles with Dendritic Groups: Effects on Physical and Biological Properties

(Spine Title: Functionalization of Polymer Vesicles with Dendritic Groups)

(Thesis Format: Monograph)

By

Ryan C. Amos

Graduate Program in Biomedical Engineering

Submitted in partial fulfillment

of the requirements for the degree of

Master of Engineering Science

The School of Graduate and Postdoctoral Studies

University of Western Ontario

London, Ontario, Canada

October, 2011

THE UNIVERSITY OF WESTERN ONTARIO

SCHOOL OF GRADUATE AND POSTDOCTORAL STUDIES

CERTIFICATE OF EXAMINATION

Supervisor

Dr. Elizabeth R. Gillies

Supervisory Committee

Dr. Len Luyt

Dr. Wankei Wan

Examiners

Dr. Maria Dangova

Dr. Len Luyt

Dr. Lynne-Marie Postovit

The Thesis by

Ryan C. Amos

entitled:

Surface Functionalization of Polymer Vesicles with Dendritic Groups: Effects on Physical and Biological Properties

Is accepted in partial fulfillment of the

requirements for the degree of

Master of Engineering Science

Date

Chair of the Thesis Examination Board

Abstract

Polymer vesicles (polymersomes) are spherical assemblies with aqueous cores, formed by the self-assembly of amphiphilic polymers in an aqueous environment. They resemble phospholipid vesicles, but typically exhibit much greater stabilities. The chemical versatility of the polymer synthesis makes it possible to tune the vesicle characteristics such as vesicle size and circulation time *in vivo*. As such, they are highly promising materials for various applications including drug delivery. Our research group recently developed a versatile approach for the conjugation of dendritic groups to the surfaces of polymer vesicles which allows the surface properties to be readily tuned for specific biological properties or applications. This thesis will investigate the effects of different dendron functionalities, both neutral and cationic, on the rate of release of encapsulated small molecules and larger biomacromolecules, cytotoxicity and the cell uptake properties of polymer vesicles. These properties were explored in both non-biodegradable vesicles based on polybutadiene-poly(ethylene oxide) (PBD-PEO) and biodegradable vesicles based on polycaprolactone-poly(ethylene oxide) (PEOPCL). The rate of release of an encapsulated small molecule, rhodamine B, was found to be dependent on the absence or presence of dendritic functionality. Unlike with small molecules, the release of encapsulated protein, bovine serum albumin (BSA), depends on the charge of the dendritic functionalization since both cationic systems exhibited faster, similar release profiles. The cytotoxicity of the vesicle systems was found to be dependent on their surface charge as toxicity was observed with both cationic systems at higher concentrations. Finally, the cell uptake was found to be dependent on the functional group displayed on the vesicle surface and guanidine functionalized vesicles had significantly increased cell uptake relative to the other samples.

Keywords: Polymer Vesicles, Self-assembly, Release, Cytotoxicity, Cell Internalization,

Statement of Co-Authorship

As the first author I was responsible for completing the literature review, dendron synthesis, PBD-PEO functionalization, click reactions of both vesicle systems, vesicle characterization, release of encapsulated small molecule and protein, cytotoxicity and cell uptake experiments. Ali Nazemi was responsible for synthesizing and preparing PEO-PCL vesicles with 20% azide loading.

The results of this monograph will be submitted for one publication. The co-authors on the manuscript will be Ali Nazemi, Dr. Colin Bonduelle and finally my graduate supervisor Dr. Elizabeth R. Gillies.

Acknowledgements

I would like to thank my graduate supervisor Dr. Elizabeth Gillies for giving me this great opportunity to conduct research on polymer vesicles, as well for her guidance and support while completing my degree. Her knowledge and dedication to research has made my time in her group rewarding.

I would also like to thank Dr. Colin Bonduelle and Ali Nazemi for their help working with me on my research project. Without their help and support, I would not have been able to complete my research. Additionally, I would like to recognize Karen Nygard for all her assistance with fluorescent microscopes and image analysis software. Furthermore, I would to thank all the members, past and present, of the Gillies group for makng my day to day life enjoyable while conducting research.

Finally, I would like to thank all my friends and family for supporting me throughout my time at Western.

Table of Contents

Page

CERTIFICATE OF EXAMINATION ii

Abstract iii

Statement of Co-Authorship iv

Acknowledgements v

List of Schemes ix

List of Tables ix

List of Figures x

List of Abbreviations xiii

Part One: Introduction 1

1.1 Drug Delivery 2

1.2 The Cell Membrane 2

1.3 Phospholipids and the Phospholipid Bilayer 4

1.4 Liposomes 5

1.5 Block Copolymers 6

1.6 Polymer Self-Assembly 6

1.7 Micelles 8

1.8 Vesicles 9

1.9 Comparison of Polymer Vesicles and Liposomes 10

1.10 Polymer Selection 11

1.11 Modes of Vesicle Preparation 12

1.12 Hydrophilic Drug Loading 13

1.13 Hydrophobic Drug Loading 15

1.14 In Vitro Analysis 16

1.15 In Vivo Analysis 18

1.16 Vesicle Surface Functionalization 18

1.17 Dendritic Surface Functionalization of Polymer Vesicles 19

1.18 Cell Penetrating Agents 20

1.19 Thesis goals 22

Part Two: Results and Discussion 24

2.1 Synthesis 25

2.1.1 Synthesis of Dendrons 25

2.1.2 Synthesis of dye-labeled dendrons 26

2.1.3 Polymer Functionalization 27

2.2 Vesicle Preparation 28

2.2.1 Vesicle Formation 28

2.2.2 Surface Functionalization of Vesicles with Dendritic Groups 29

2.2.3 Quantification of Dendron Conjugation 34

2.3 Encapsulation and Release of Small Molecules and Proteins 36

2.3.1 Encapsulation and Release of Rhodamine B 36

2.3.2 Encapsulation and Release of Rhodamine labeled BSA 42

2.4 Cell Viability 47

2.5 Cell Uptake 52

Part Three: Conclusion 57

3.1 Conclusion 58

Part Four: Experimental 60

4.1 Experimental 61

4.2 General Procedure for the Preparation of PEO-PBD Vesicles 61

4.3 General Procedure for the Preparation of PEO-PCL Vesicles 61

4.4 General Procedure for Surface Functionalization of Vesicles 62

4.5 Quantification of Surface Dendritic Groups 62

4.6 Encapsulation and Release of Small Molecules from Vesicles 62

4.7 Encapsulation and Release of Protein from Vesicles 63

4.8 Procedure for MTT assay 64

4.9 Cell Uptake 64

Part Five: References 66

Curriculum Vitae 72

List of Schemes

Page

Scheme 1. Divergent synthesis of a third generation polyester dendron. 25

Scheme 2. Functionalization of a third generation dendron from hydroxyl functionality to amine and guanidine functionality..... 26

Scheme 3. Synthesis of Rhodamine labeled guanidine dendron. 27

Scheme 4. Surface functionalization of polymer vesicles via click reaction. 30

List of Tables

Page

Table 1. Conjugation efficiency of amine and guanidine dendrons to the surface of polymer vesicles..... 35

Table 2. Coefficients of curve-fit from Kaleida Graph 4.0 for a first-order model. 39

Table 3. Coefficients of curve-fit from Kaleida Graph 4.0 for a power law model..... 44

List of Figures

Page

Figure 1. Schematic of the cell membrane.[7] 4

Figure 2. Schematic of a liposome, hydrophilic head groups seen in green and hydrophobic tails in purple.....5

Figure 3. Schematic of block copolymer composition with corresponding assembled structure...7

Figure 4. Cross-sectional schematic of liposomes (left) and polymer vesicles (right). Grey indicates hydrophobic region and light blue indicates hydrophilic region.[17].....10

Figure 5. Surface functionalization of polymer vesicles with dendritic groups via click chemistry.[34].....19

Figure 6. Postulated mechanism of direct cell penetration of cargo conjugated to a dendron with guanidine functional groups on the periphery.[2].....21

Figure 7. Self-Assembly of 20% azide functionalized PBD-PEO and PEO-PCL vesicles.....28

Figure 8. Size distribution of vesicle sample **10** expressed as a volume fraction.....30

Figure 9. Size distribution of vesicle sample **12** expressed as a volume fraction.....31

Figure 10. Size distribution of vesicle sample **13** expressed as a volume fraction.....31

Figure 11. Size distribution of vesicle sample **14** expressed as a volume fraction..... 33

Figure 12. Size distribution of vesicle sample **11** expressed as a volume fraction..... 34

Figure 13. Size distribution of vesicle sample **15** expressed as a volume fraction..... 34

Figure 14. Release of encapsulated rhodamine B expressed as percent released from vesicle sample **10**. The data was fit to a first-order model. 39

Figure 15. Release of encapsulated rhodamine B expressed as percent released from vesicle sample **12**. The data was fit to a first-order model. 40

Figure 16. Release of encapsulated rhodamine B expressed as percent released from vesicle sample **13**. The data was fit to a first-order model. 40

Figure 17. Release of encapsulated rhodamine B expressed as percent released from vesicle sample **14**. The data was fit to a first-order model. 41

Figure 18. Release of encapsulated rhodamine B expressed as percent released from vesicle sample **11**. The data was fit to a first-order model. 41

Figure 19. Release of encapsulated rhodamine labeled BSA expressed as percent released from vesicle sample 10. The data was fit to a power-law model. 44

Figure 20. Release of encapsulated rhodamine labeled BSA expressed as percent released from vesicle sample **12**. The data was fit to a power-law model. 45

Figure 21. Release of encapsulated rhodamine labeled BSA expressed as percent released from vesicle sample **13**. The data was fit to a power-law model. 46

Figure 22. Release of encapsulated rhodamine labeled BSA expressed as percent released from vesicle sample **14**. The data was fit to a power-law model. 46

Figure 23. Release of encapsulated rhodamine labeled BSA expressed as percent released from vesicle sample **11**. The data was fit to a power-law model. 47

Figure 24. Toxicity profile of vesicle sample **10** as measured by the MTT assay. Error bars represent 1 standard deviation from the mean. 48

Figure 25. Toxicity profile of vesicle sample **12** as measured by the MTT assay. Error bars represent 1 standard deviation from the mean. 49

Figure 26. Toxicity profile vesicle sample **13** as measured by the MTT assay. Error bars represent 1 standard deviation from the mean. 49

Figure 27. Toxicity profile of vesicle sample **14** as measured by the MTT assay. Error bars represent 1 standard deviation from the mean. 50

Figure 28. Toxicity profile of vesicle sample **11** and vesicle sample **15** as measured by the MTT assay. Error bars represent 1 standard deviation from the mean. 51

Figure 29. Confocal Microscope image of HeLa cells incubated with vesicle samples **10** (top left), **12** (top right), **13** (bottom left) and **14** (bottom right) at a concentration of 0.25 mg/mL with 1% rhodamine B dye labeled polymer. DAPI is seen in blue and rhodamine in red..... 53

Figure 30. Intensity analysis of vesicle samples **10**, **12**, **13** and **14**. Error bars represent one standard deviation from the mean..... 54

Figure 31. Confocal Microscope image of HeLa cells incubated with vesicle samples **11** (left) and **15** (right) at a concentration of 0.25 mg/mL with 1% rhodamine B dye labeled polymer. DAPI is seen in blue and rhodamine in red. 55

Figure 32. Intensity analysis of vesicle samples **11** and **15**. 56

List of Abbreviations

AON	Antisense Oligonucleotide
Boc	t-butyl carbonate
BSA	Bovine Serum Albumin
ConA	Concanavalin A
DAPI	4, 6-diamidino-2-phenylindole
DI	Deionized
DIPEA	Diisopropylethylamine
DMAP	4-dimethylaminopuridine
DMSO	Dimethyl Sulphoxide
EPR	Enhanced permeability and retention
FITC	Fluorescein Isothiocyanate
HBTU	*O*-(benzotriazol-1-yl)-*N*,*N*,*N*',*N*'-tetramethyluronium hexafluorophosphate
HIV	Human Immunodeficiency Virus
HOBt	Hydroxybenzotriazole
HSD	Honestly Significant Difference
MeOH	Methanol
mRNA	Messenger RNA
MTT	3-(4,5-Dimethylthiazol-2-yl)-2,5-diphenyltetrazolium bromide
MWCO	Molecular Weight Cut-Off
PBD-PEO	Polybutadiene-b-Poly(ethylene oxide)
PBD-PEO-N_3	Azide Terminated Polybutadiene-b-Poly(ethylene oxide)
PBS	Phosphate Buffered Saline
PCL	Polycaprolactone
pdi	Polydispersity Index

PEO	Poly(ethylene oxide)
PEO-PCL	Polycaprolactone-b-Poly(ethylene oxide)
RNAi	RNA Interference
siRNA	Short Interfering Ribonucleic Acid
TEM	Transmission Electron Microscopy
TFA	Trifluoroacetic Acid
ε	Extinction Coefficient

Part One: Introduction

1.1 Drug Delivery

Developments in biology and chemistry have led to a wide variety of therapeutics that are available to treat diseases at the cellular level. Some of these therapeutics include small molecules, peptides, proteins, antibodies and nucleic acid derivatives.[1] One of the largest hurdles to overcome in treating disease is to deliver a target molecule to the actual target cells, and then into the target cell past the cell membrane.[2] To accomplish this, the desired therapeutic must be able to travel within the blood stream, which is composed primarily of water. Having hydrophilic characteristics is advantageous for traveling in the bloodstream but once the therapeutic reaches its desired site it must also pass the cell membrane. The cell membrane is hydrophobic in nature and hydrophilic molecules encounter challenges in passing through the membrane unless there is an active uptake pathway. Hydrophobic molecules, such as cholesterol, can move freely in cell membranes but have poor water solubility. An ideal therapeutic must exhibit a balance between hydrophobicity and hydrophilicity.

In addition to an inability to cross the cell membrane, short circulation times in the blood, undesired rapid biodegradation of biomolecules, and lack of specificity for the therapeutic target are also common limitations of drug candidates. New nanoscale delivery systems allow for delivery of therapeutics in a form in which they are physically protected from degradation by the body, and may exhibit increased circulation time, targeted delivery to decrease potential harmful side effects and finally, provide a controlled release mechanism of delivery.[3]

1.2 The Cell Membrane

The cell membrane has evolved to protect the cell from the exterior environment and to retain essential molecules within the cell.[4] The membrane is selectively permeable to ions, such as sodium and potassium, and to small molecules such as water, which pass through via

transporter proteins. The cell membrane is composed primarily of a phospholipid bilayer with proteins and glycoproteins imbedded in the bilayer, as shown in Figure 1. Glycoproteins are composed of a globular protein which has undergone a post-translational modification to be covalently bound to a sugar backbone. These proteins are involved in cellular signaling, cell-cell interactions and provide a scaffold for targeting. The cell membrane is involved in several pathways within the cell to facilitate survival activities such as cell adhesion and cell signaling. Recycling of the cell membrane is an essential process which is accomplished by two complimentary mechanisms, exocytosis and endocytosis.[5] Exocytosis involves fusion of intracellular vesicles to the surface of the cell membrane; this provides a mechanism of excreting/removing material and installing new proteins on the membrane surface. Endocytosis is the reverse of exocytosis; the process provides the cell with a mechanism to internalize molecules in the extracellular matrix that cannot pass through the cell membrane, and removes proteins from the surface of the membrane. As these processes are dependent on the fluidity of the membrane, they can be inhibited by decreasing the temperature of the system. At lower temperatures, the cell membrane becomes more crystalline and formation of vesicles composed of a lipid bilayer becomes thermodynamically unfavourable.[6]

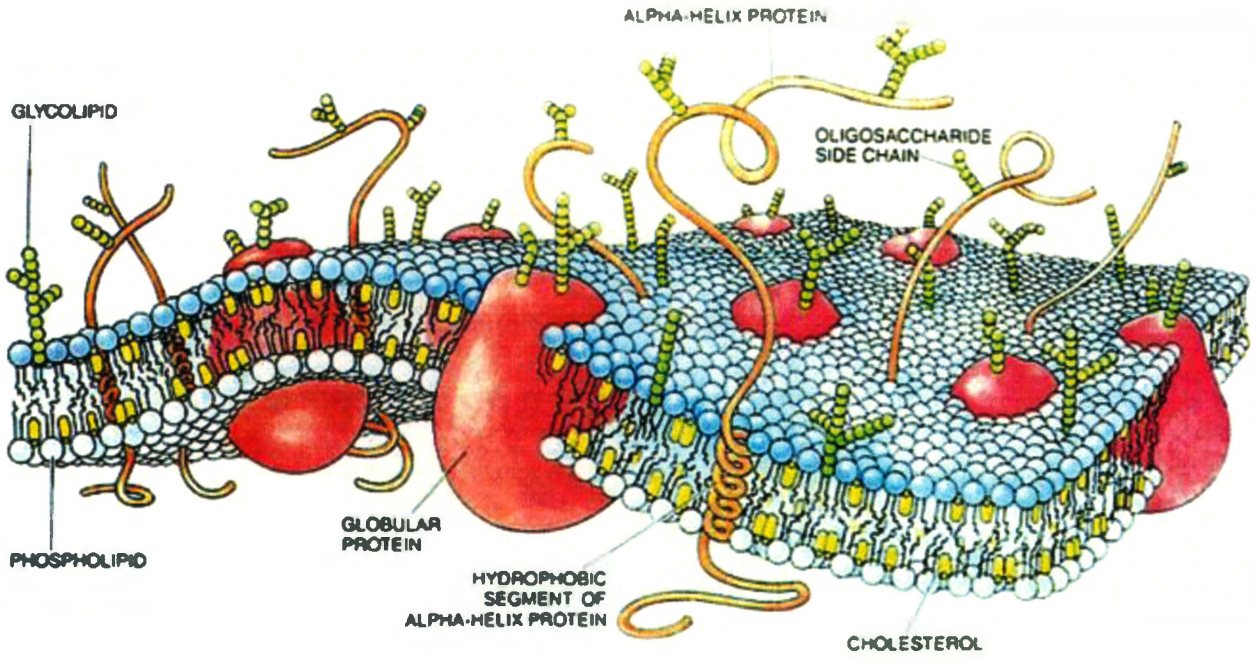

Figure 1. Schematic of the cell membrane.[7] The drawing was made by Dana Burns, and can also be found in Scientific American, 1985, 253(4), pages 100-108, in the article *The molecules of the cell membrane* by M.S. Bretscher.

1.3 Phospholipids and the Phospholipid Bilayer

Comprising the cell membrane, phospholipids are capable of forming a bilayer due to their amphiphilic structure. Phospholipids are composed of a hydrophilic "head" group with a phosphate and sometimes other hydrophilic molecules attached to the phosphate group. The polar head group is attached to the hydrophobic region by a glycerol group. The hydrophobic "tail" region is composed of two fatty acid chains. In aqueous conditions, the hydrophobic fatty acid chains align together away from water while the hydrophilic phosphate group is dissolved in water.

The amphiphilic nature of the phospholipids allows for spontaneous assembly into a bilayer with the tails aligning, forming a hydrophobic membrane interior, while the hydrophilic

heads remain solvated in an aqueous environment. The hydrophobic tail region of the bilayer is stabilized by hydrophobic interactions between different fatty acid chains. The longer the fatty acid chains in the bilayer, the stronger the interaction.[8] Furthermore, hydrophobic alignment prevents water molecules from forming a solvating shell, which decreases the free energy of the system thus making it less thermodynamically favourable.[8] A common drug delivery system which utilizes characteristics of the cell membrane is liposomes.[9]

1.4 Liposomes

Liposomes are composed of synthetic phospholipids which spontaneously assemble into a vesicle structure, as seen in Figure 2, enabling target drugs to be encapsulated during assembly.[10] Drugs which would be harmful to the body can be encapsulated and delivered specifically to a target site such as a tumor or diseased tissue, decreasing the toxicity to the body. There are three different types of liposomes: multilamellar vesicles,[11] small unilamellar vesicles [12] and large unilamellar vesicles.[13] Furthermore, the surface of the liposome can be functionalized to produce a targeted liposome.[14] Currently, liposome delivery systems are commercially available including Doxil, Epaxal and Myocet.

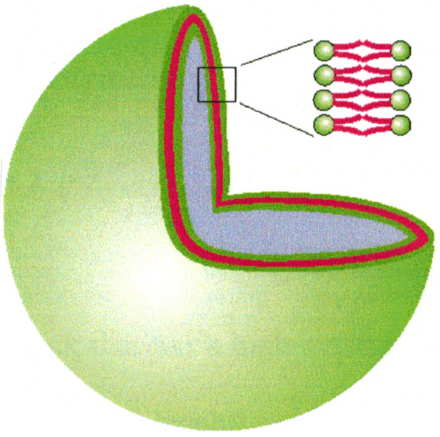

Figure 2. Schematic of a liposome, hydrophilic head groups seen in green and hydrophobic tails in purple.

Despite the advantage of being composed of phospholipids commonly found in the cell membrane, liposomes have several limitations. The small tail region of the phospholipid molecule impedes the high loading of hydrophobic drugs, limiting liposomes to only load hydrophilic drugs efficiently.[15] Furthermore, the small tail region provides a small hydrophobic barrier which results in encapsulated drugs within liposomes leaking out quickly, decreasing the overall efficiency of delivery.[16] Finally, circulation times of liposomes are short as there are several mechanisms within the body to remove liposomes from the blood.[17]

1.5 Block Copolymers

Block copolymers are composed of a unit of polymerized monomers attached to at least one other unit of different polymerized monomers.[18] Block copolymers are characterized by the number of blocks they are composed of; a block copolymer consisting of two blocks is called a diblock copolymer while a copolymer consisting of three blocks in either an ABA or ABC orientation, where A, B and C are different polymer blocks, is called a triblock copolymer. Having different polymer units bound together allows for tunability of a polymer of interest, like thermostability,[19] elasticity[20] or solubility.[21] Copolymers that contain hydrophilic regions and hydrophobic regions have similar stereoelectronics as phospholipids. As a result, these block copolymers exhibit self-assembly characteristics.[22]

1.6 Polymer Self-Assembly

Block copolymers that assemble into ordered aggregates in water contain a hydrophilic block that has a high solubility in water. Poly(ethylene oxide) (PEO) is a common polymer used as the hydrophilic block.[22] The volume fraction of the hydrophilic block relative to the hydrophobic block in the solvent dictates which morphology the assembly will take.[23] As shown in Figure 3, generally, if the hydrophilic volume fraction is greater than 50%, a spherical micelle

assembly will form. The core of the micelle will be composed of the hydrophobic block of the copolymer and the exterior shell will be composed of the hydrophilic block. If the volume fraction of the hydrophilic block is between 40-50%, a wormlike-micelle will often form with the core being composed the hydrophobic block and the cylinder shell being composed of the hydrophilic block. Finally, if the volume fraction of the hydrophilic block is between 25-40% a vesicle structure with a core composed of the solvent and a shell composed of the hydrophobic block can form. The hydrophobic monomer unit does not generally influence the morphology the copolymer will assemble into, rather influences the stability of the assembly.[17]

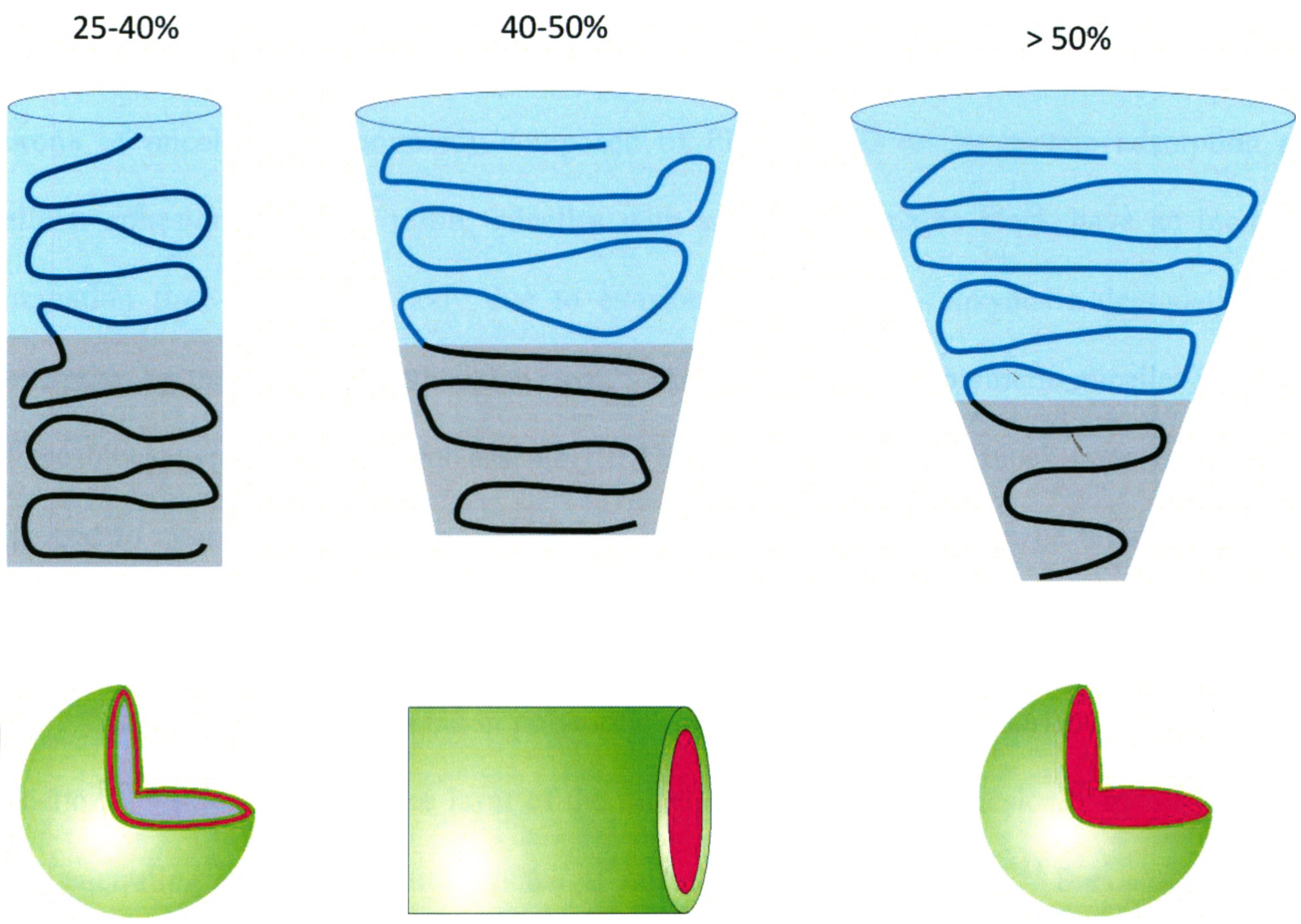

Figure 3. Schematic of block copolymer composition with corresponding assembled structure.

1.7 Micelles

Polymeric micelles form from block copolymers that have a hydrophilic volume fraction greater than 50% relative to the hydrophobic region. There are several advantages to using micelles in drug delivery, including dissolution of hydrophobic drugs and increased circulation times in the bloodstream. Micelles are capable of physically entrapping hydrophobic molecules in the hydrophobic core.[18] The entrapped molecules are protected from the external environment by the hydrophilic corona of the micelle. Due to this, improvements in drug solubility of several orders of magnitude can be obtained by using micelles relative to direct dissolution.[24] Furthermore, as the hydrophobic drug is protected within the core and away from the blood, there is less chance of the drug being metabolized by the body before delivery. The hydrophilic corona of micelles are commonly composed of PEO.[25] PEO resists protein adsorption and cellular adhesion.[17] As a result, micelles with a PEO hydrophilic block have an increased circulation time within the body due to evasion of hydrolysis, enzymatic degradation and absorption by the reticuloendothelial system.[26] Another feature of polymeric micelles is control of the block copolymer used for assembly. The composition of the block copolymer can be changed to alter degradation time within the body and chain length can be altered to control diameter of the micelle as well as the morphology of the micelle.[27]

More recent advancements in polymeric micelles are to alter the surface topology of the micelle.[27] While a PEO surface layer of the micelle resists cellular adhesion,[17] by addition of a cell-penetrating agent the cellular uptake of micelles could be increased.[27] Previously, micelle targeting has depended on a passive targeting technique termed the enhanced permeability and retention (EPR) effect for delivery to tumour tissues.[25] This EPR effect results from vasculature in tumour tissue which has a discontinuous endothelium. As well, the lymphatic drainage system

is not completely developed. As a result, assembled polymer systems accumulate in the tissue around this vasculature system.[28] Active targeting can be achieved by functionalizing the surface of the micelle with a molecule that will bind to cellular receptors on the cell membrane of the target cell. For example, Chilkoti and coworkers prepared polypeptide micelles that had been functionalized with the tripeptide targeting group asparagine-glycine-arginine which targets the transmembrane protein CD13 which is unregulated in tumour vasculature.[29] They found that the functionalized micelles accumulate more in tumour vasculature compared to non-cancerous tissue. As well, the functionalized micelles accumulate more in tumour vasculature as compared to unfunctionalized micelles. However, despite their positive results, they claimed their system was far from optimized.[29]

Despite all the advantages of micelles, they are only efficient for delivery of hydrophobic drugs. If a charged or hydrophilic drug needs to be delivered to a certain site within the body another drug delivery system must be employed.

1.8 Vesicles

Polymer vesicles, commonly referred to as polymersomes by analogy with liposomes, generally form in water from block copolymers with a hydrophilic volume fractions between 25-40%.[22] Diblock copolymers that assemble into vesicles form a polymeric bilayer that is similar in orientation to a phospholipid bilayer. Triblock copolymers with an orientation of ABA where A is the hydrophilic block and B is the hydrophobic block will form a polymeric monolayer. Triblock copolymers with a composition of ABC where A is the hydrophilic block, B is a hydrophobic block and C is a different hydrophobic block will assemble into vesicles with a polymeric bilayer similar in orientation to diblock copolymers.

1.9 Comparison of Polymer Vesicles and Liposomes

There are both similarities and dissimilarities between polymer vesicles and liposomes. The two systems are similar in that they are both composed of amphiphiles and both spontaneously assemble into spherical objects with an aqueous lumen. Furthermore, they both have a hydrophobic membrane, as seen in Figure 4, which separates the lumen from the exterior.[17] For encapsulated molecules to escape the lumen they must travel through the hydrophobic region or a pore must open for the molecules to escape. Finally, both have the potential for the outer layer to be functionalized with a molecule of interest, such as a targeting group or a cell penetrating agent.

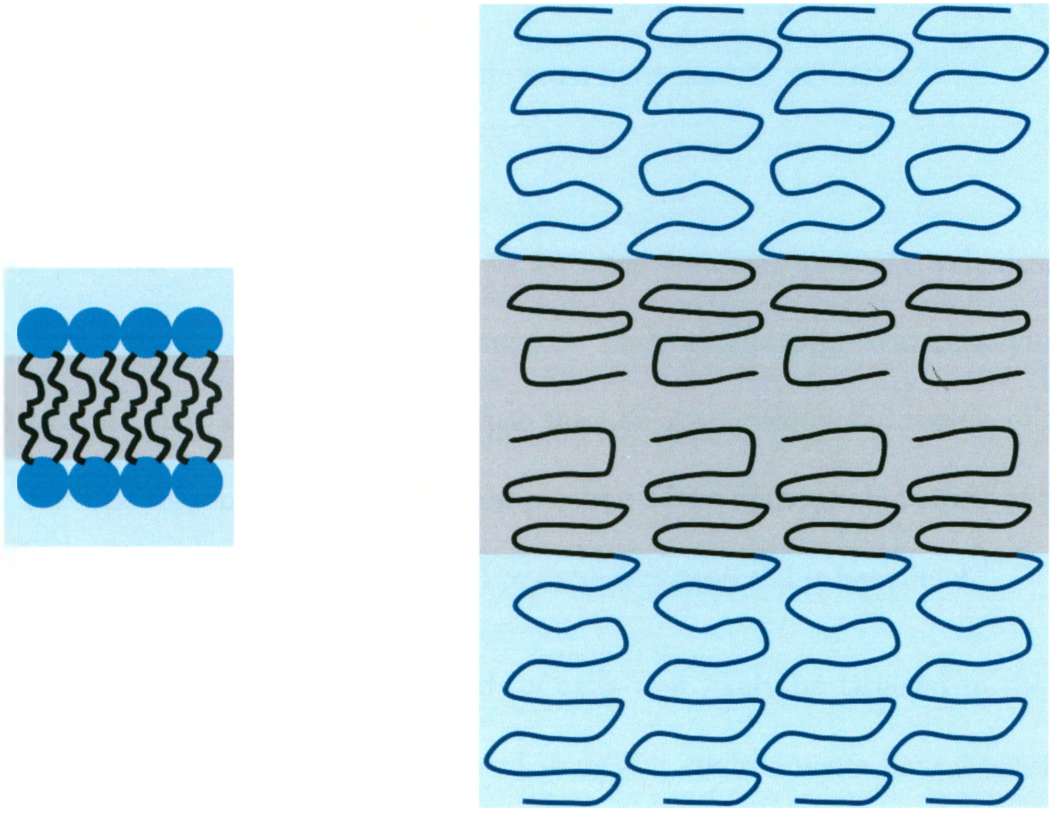

Figure 4. Cross-sectional schematic of liposomes (left) and polymer vesicles (right). Grey indicates hydrophobic region and light blue indicates hydrophilic region.

While liposomes and polymer vesicles both have a defined membrane structure, the liposome's hydrophobic region tends to be approximately 3 nm in width while polymer vesicles' hydrophobic region can exhibit a width from 8-20 nm depending of the length of the polymer.[17] The advantage of having a larger hydrophobic region is that there is a greater loading capacity for hydrophobic molecules in the membrane as well as a decreased rate of diffusion through the membrane for encapsulated hydrophilic molecules.[23] Moreover, the copolymer used for assembly can alter characteristics of the vesicle. Stimuli-responsive polymers, which degrade in response to external cues such as pH or oxidative potential, provide an escape mechanism for encapsulated hydrophilic molecules in the lumen or hydrophobic molecules. By providing a release mechanism, polymer vesicles can deliver their cargos to specific sites while keeping non-specific delivery to a minimum, a characteristic most liposomes do not have.[30]

1.10 Polymer Selection

Since polymer vesicles are desired to be used for drug delivery vehicles, a release mechanism from polymer vesicles is advantageous. Hydrophilic cargo within polymer vesicles are trapped because they cannot readily diffuse through the hydrophobic region of the vesicle membrane. For that reason, controlling the composition of the hydrophobic block of copolymers so they respond to external stimuli such as pH or oxidative potential is beneficial.[30]

Polymer vesicles that are internalized by cells will likely be targeted to the lysosome. With that in mind, copolymers which respond to acidic environments have become popular. Incorporation of 2-(diethyl amino)ethyl methacrylate into the hydrophobic block of assembling copolymer allows control over the permeability of the vesicle membrane. In acidic environments, like those found in endolysosomes, 2-(diethyl amino)ethyl methacrylate becomes

protonated, resulting in a shift from hydrophobic to hydrophilic character. As a result, pores form in the vesicle membrane which allow for release of encapsulated cargo.[31]

The endolysosome environment not only has a different pH than the cytoplasm, but also has a higher oxidative potential.[32] Copolymers which degrade under these conditions would be advantageous for targeted release. Hubbell and coworkers synthesized a copolymer with a disulfide bond between the hydrophilic PEO block and the hydrophobic poly(propylene sulfide) block. They report that the resulting vesicles rupture within 10 minutes in the endolysosomal environment due to cleavage of the disulfide bond between the hydrophilic and hydrophobic block.[32]

While there are mechanisms to induce release from polymer vesicles, new systems are continually being reported utilizing different parameters such light or temperature. When choosing the composition of copolymers multiple variables must be considered such as biocompatibility, release mechanism, circulation time and vesicle loading. While composition of the copolymer is important, it is not the only parameter that needs to be controlled.

1.11 Modes of Vesicle Preparation

Self-assembly of block copolymers into supramolecular structures usually proceeds through one of two methods, either dissolution of the copolymer into an organic solvent and then addition of water, or dissolution directly into water.[30] The first method, often referred to as "solvent-switch," requires the copolymer be dissolved in an organic solvent that is miscible with water.[27] As the copolymer has a large hydrophobic region, it is unlikely that the copolymer can dissolve directly into water. Upon the addition of water, the hydrophobic blocks of the copolymer begin to associate with each other in the hydrophilic environment. However a

drawback of solvent switching is that after assembly the organic solvent has to be removed by dialysis, which can be time consuming.[33]

The second, direct solution method, involves hydration of the pure copolymer from a film.[34] To produce a film, the copolymer is often dissolved in an organic solvent and then the solvent is removed by evaporation. As an organic solvent is usually used, it is not a true organic solvent free method although there is no mixing between the organic solvent used and water used in the assembly. Vesicles begin to form upon hydration of the film. Film rehydration requires aggressive stirring and longer preparation times as compared to the solvent switch. Furthermore, this method tends to lead to higher vesicle polydispersities. However, while solvent switch methods require dialysis to remove remaining organic solvent, organic solvent free methods do not require dialysis.[35]

New methods are being developed for self-assembly to improve loading efficiency but ultimately use at least one of the above methods in some degree. For instance, Weitz and coworkers have developed a method for preparing vesicles with 100% encapsulation efficiency using a water/oil/water emulsion and a microfluidic device while controlling the size of the formed vesicles.[36] As well, their model can be applied to form polymer vesicles within polymer vesicles and higher order polymer vesicle systems.[37]

1.12 Hydrophilic Drug Loading

Due to the presence of an aqueous lumen in polymer vesicles, hydrophilic molecules can be encapsulated.[22] Small molecules dissolved in the water used for vesicle preparation will be encapsulated within the polymer vesicle. The concentration of small molecules will be the same inside the vesicle as outside the vesicle; this results from a physical encapsulation of the aqueous

solution. Non-encapsulated molecules can subsequently be removed by dialysis or another size based technique. To obtain higher loadings, a thermodynamic driving force must be used, such as manipulating pH gradients.[15] Furthermore, encapsulation of hydrophilic molecules is not limited to small molecules. Larger molecules, such as proteins, can be encapsulated as shown by Discher and coworkers.[38]

The fluorescently labeled insulin is contained completely within the polymer vesicle. The overlay of the two channels, red for the polymer membrane and green for insulin, indicates that the membrane extends further than insulin. Furthermore, the most intense region of the polymer is at the outer edge, consistent with PKH26 staining the membrane. The insulin does not overlap with the brightest region, the membrane, suggesting that it is in the lumen and does not associate with the hydrophobic membrane.

Discher and coworkers showed that other biological macromolecules could be encapsulated within the lumen of polymer vesicles. Short interfering ribonucleic acid (siRNA) knockdown gene products by initializing cell RNA interference (RNAi) pathways in the cytosol whereas antisense oligonucleotides alter splicing of messenger RNA (mRNA) transcripts.[39] To achieve encapsulation, copolymer dissolved in dimethyl sulphoxide (DMSO) was added to aqueous solutions of either FITC-siRNA or FITC-antisense oligonucleotide (AON). Dialysis with a 3.5 KDa molecular weight cut-off (MWCO) membrane was used to remove residual DMSO followed by dialysis using a 300 KDa MWCO membrane to remove non-encapsulated material.

Similar to protein encapsulation, both FITC-AON and FITC-siRNA are localized exclusively within the lumen of the polymer vesicle since the overlay image cleary indicates that

polymer extends beyond the colocalized region of the polymer and nucleic acids. In addition, as the most intense region of polymer, the membrane, does not show colocalization with the nucleic acids, it can be concluded that the nucleic acids are in the lumen and do not associate with the hydrophobic membrane.

1.13 Hydrophobic Drug Loading

Hydrophobic loading into the polymeric membrane has been previously demonstrated. However, a drawback was that the hydrophobic model molecule did not have a full hydrophobic character. Maskos and coworkers showed encapsulation of a completely hydrophobic dye (Nile Red) into the membrane of the vesicle as well as incorporation of quantum dots into the membrane without changing the size of the vesicle.[40]

Furthermore, Discher and coworkers showed encapsulation of a hydrophobic drug, paclitaxel, and a hydrophilic drug, doxorubicin, within polymer vesicles.[41] The hydrophobic paclitaxel was sequestered within the polymer membrane while the hydrophilic doxorubicin was located in the aqueous core of the vesicle. The advantage of having a system with both drugs encapsulated would be to ensure that the cells which internalize the vesicle would be subjected to both anticancer agents. As both drugs would be in the cell, there should be higher cytotoxicity as well as a decreased chance of the cancerous tissue becoming resistant to one or both drugs. Furthermore, biodegradable copolymers, based on of polycaprolactone (PCL) and poly(lactic acid), were incorporated into the polymer vesicles to aid in release of the drugs from the vesicles following internalization.

1.14 In Vitro Analysis

To illustrate their dual drug encapsulation system, Discher and coworkers performed cell uptake experiments on human breast cancer cells using a biodegradable and non-biodegradable polymer vesicle system. The results can be seen in Figure 10.

With the biodegradable system, encapsulated doxorubicin was able to leave the vesicle and concentrate in the nucleus. The polymer is seen in green and little colocalization was observed with doxorubicin. By doing so, doxorubicin is available to exert its therapeutic effects within the cell by ultimately halting the cell cycle and killing the cancerous cell. With the non-biodegradable system, doxorubicin is colocalized with the polymer vesicle. While in the vesicle and not in the nucleus, doxorubicin would not be able to exert its effect within the nucleus. Therefore, the effectiveness of the delivery system is limited by the release of the encapsulated cargo post internalization. Furthermore, the polymer appears punctate around the nucleus but not within the nucleus, which suggests that the vesicles are localized within endolysosomal cavities. However, further investigation is required to draw a conclusion.

To investigate cellular internalization and localization of polymer vesicles, Kamei and coworkers co-stained different cellular organelles to determine the fate of polymer vesicles after internalization.[6] For their study, vesicles were prepared from a copolymer composed of polyarginine as the hydrophilic block and polyleucine as the hydrophobic block. This composition had been shown to increase cell internalization.[42] Before uptake with vesicles, the HeLa cells were incubated with antibodies for either early endosomes or lysosomes. After uptake, secondary antibodies with a fluorescent tag (Cy5) were used to visualize the different cellular compartments. The results of the uptake experiment can be seen in Figure 11.

Arginine-Leucine polymer vesicles are located within early endosomes after internalization as seen by colocalization of the polymer (green) with the endosomes(red) in Figure 11. However, vesicles appear to avoid lysosomes. As the vesicles avoid lysosomes, therapeutics such as proteins and siRNA that may degrade in the harsh environment of the lysosome can be employed without worry of premature degradation. However, the localization of the vesicles in early endosomes indicates that for effective delivery of therapeutics to target cells, there must be a release mechanism built into the vesicles, such as incorporation of biodegradable copolymers. If there is not a release mechanism, vesicles could be recycled back to the cell surface and sent out of the cell without delivering its payload and ultimately be cleared from the host.

As it has been shown that vesicles do not concentrate in lysosomes, Discher and coworkers showed that their encapsulated siRNA system would trigger a biological response in vitro.[39] If vesicles concentrated in lysosmes, sensitive molecules, such as siRNA, would degrade before being able to interact with other molecules in the cytosol or cellular organelles. As well, siRNA is charged and has difficulty crossing the cell membrane. Once encapsulated the charge is hidden from the cell membrane. To study their system, polymer vesicles with encapsulated siRNA designed to knockdown lamin A/C protein was compared with free siRNA, siRNA encapsulated in liposomes (LF2k) and viral delivery (Lenti-shRNA).

Polymer vesicles with encapsulated siRNA appear to be as effective as commercially available liposomes with encapsulated siRNA. Furthermore, the polymer vesicle system is visibly more effective at delivering siRNA into the cell in comparison with free siRNA. However, commercially available viral systems are more efficient at delivering siRNA into the

cell. This suggests that internalization is not just a passive mechanism but rather can be influenced by surface topology of the delivery system.

1.15 In Vivo Analysis

One advantage of polymer vesicles over liposomes is their circulation time in vivo. To increase the circulation time of liposomes in vivo, a PEO has been conjugated to a certain fraction of the phospholipids comprising the vesicle.[43] PEO resists protein absorption and uptake by the reticuloendothelial system.[15] Polymer vesicles that contain PEO as their hydrophilic block circulate even longer than liposomes with PEO.[17] The half life of PEO vesicles circulating are usually in the range of 20-30 hours. Polymer vesicles with PEO as the hydrophilic block selectvely accumulate in tumour sites to some extent via the EPR effect as described above.[38] However, this form of targeting is not highly specific, so some systems may need a form of active targeting.

1.16 Vesicle Surface Functionalization

A common approach for vesicle functionalization is to manipulate the terminal group of the hydrophilic block. van Hest and coworkers made copolymers with azides at their termini.[44] The azide functional group can in principle react with an alkyne moiety of another molecule of interest via a copper catalyzed "click" reaction.[44] To illustrate their model van Hest and coworkers clicked fluorescent dyes onto the surfaces of vesicles.

While active targeting of polymer vesicles would add another layer of functionality, active targeting of polymer vesicles is a relatively new area of study. Hammer and coworkers showed that polymer vesicles with biotin groups on their surfaces can bind to surfaces with avidin and also to cells with avidin on their surfaces.[45] Using their model, they attached other

proteins, like antihuman IgG, to target polymer vesicles to specific cells.[46] As well, Hunziker and coworkers attached polyguancylic acid to target macrophages with upregulated SRA1 receptor.[47] While these systems work *in vitro*, they have not been proven *in vivo*.

1.17 Dendritic Surface Functionalization of Polymer Vesicles

In the Gillies lab, a similar approach to van Hest has been reported except that the molecule attached to the surface of the vesicle is branched and multivalent.[34] A polyester dendron based on 2,2-bis(hydroxymethyl)propanoic acid and containing a focal point alkyne group was synthesized and subsequently attached to the assembled vesicle surface as seen in Figure 5. The advantage of attaching the dendron to the surface of the vesicle after assembly is that the dendron will not interfere with the self-assembly of the vesicle. The attachment of the branched dendron adds another hydrophilic block to the polymer and a different morphology, or no self-assembly, could be attained if the dendron were attached before assembly.

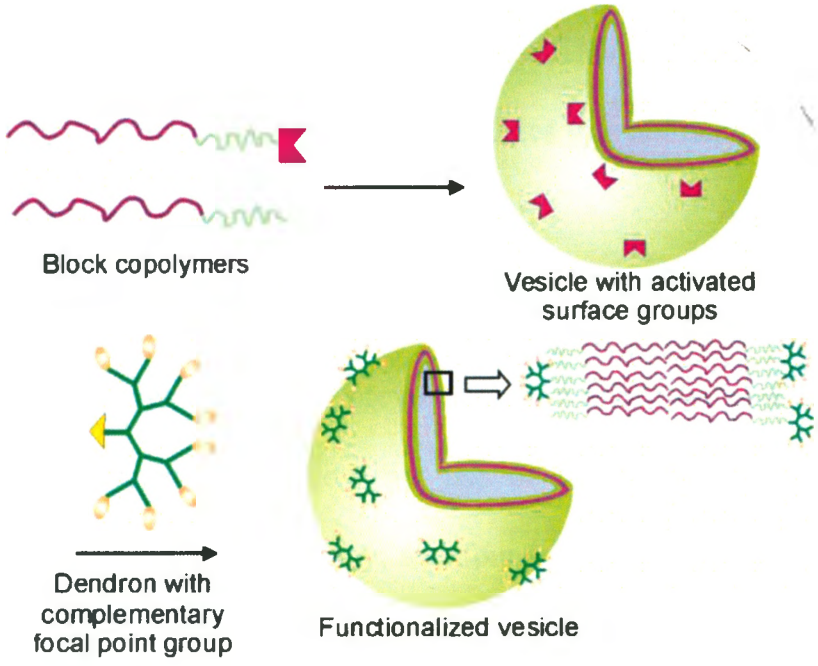

Figure 5. Surface functionalization of polymer vesicles with dendritic groups via click chemistry.

Thus far, the Gillies group has introduced dendritic groups to the surfaces of vesicles based on both nondegradable PBD-PEO copolymers[34,48] and PCL-PEO copolymers[27]. Dendrons with several peripheral functionalities such as hydroxyls, amines, and mannose molecules have been investigated and the chemistry has proven to be versatile and reproducible. In addition, using mannose as a model biological ligand, it was demonstrated that enhanced binding to the protein target concanavalin A (ConA) was obtained when vesicles were functionalized on their surfaces with dendritic mannose rather than individual molecules of mannose.[48] This was hypothesized to result from increased availability of the mannose on the vesicle surface when it was presented on the dendrimer periphery as the dendron would reside at the vesicle surface rather than being buried within the PEO layer. This study suggested that the dendritic scaffold may be ideal for the display of biological ligands in drug delivery systems. However, in this dendritic surface functionalization work it was noted that the conjugation of high levels of dendritic groups induced vesicle aggregation, possibly the result of membrane destabilization due to the branched architecture of the dendritic group. This aspect requires further study. In addition the encapsulation of molecules within the vesicles was not explored in combination with the dendritic surface functionalization approach.

1.18 Cell Penetrating Agents

While polymer vesicles have been previously shown to enter cells *in vitro* and in *vivo*, increasing the internalization would allow for use of lower clinical dosage. To increase internalization, researchers looked to biology, and found that a protein produced by the human immunodeficiency virus (HIV) has cell penetrating properties.[49] Extensive studies have revealed that the critical portion of this protein, responsible for its cell penetrating properties is a 9 amino acid sequence.[50] This sequence contains 6 arginine residues and 2 lysine residues, suggesting that

cationic charge is essential for increased internalization. Further research has shown that linear sequences of arginine residues are even more efficient at penetrating the cell membrane while linear sequences of lysine residues are less efficient than the native sequence, suggesting the guanidine group on the arginine residue is required for the increased penetration observed.[2] Furthermore, introducing flexibility into the backbone of the sequence further increases the efficiency.[51] A variety of linear and multivalent displays of guanidinium moieties have subsequently been developed and shown to exhibit cell penetrating properties.[2]

Utilizing the above principles, the Gillies lab developed a polyester dendron having eight guanidine moieties at its periphery.[51] This dendron is easy to prepare synthetically, is based on a biodegradable scaffold, and was shown to have similar cell penetrating properties to the HIV_{49-57} peptide *in vitro*.[51] It has also been demonstrated that conjugation of this Dendron to superparamagnetic iron oxide nanoparticles enhances their uptake into GL261 cells, enabling their enhanced detection by magnetic resonance imaging.[51] Furthermore, it was shown that conjugation of the same dendron to biodegradable micelles increases their internalization into HeLa cells.[27] While the exact mechanism of internalization has not been elucidated, a hypothesis of direct internalization can be seen in Figure 6.[2]

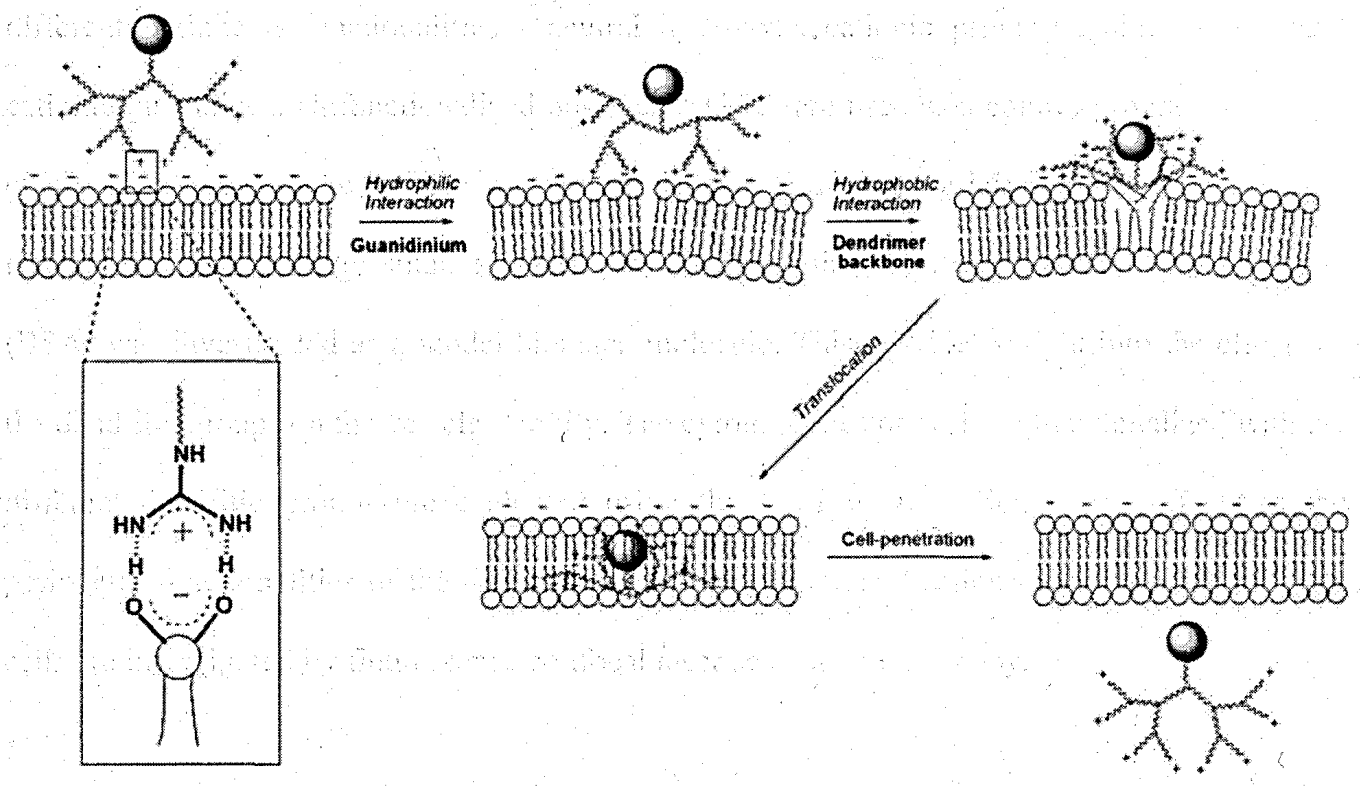

Figure 6. Postulated mechanism of direct cell penetration of cargo conjugated to a dendron with guanidine functional groups on the periphery.

While guanidine-rich cell penetrating agents have a demonstrated ability to efficiently cross cell membranes, the concentration of the cell penetrating agent must be moderated. Although extensive toxicity studies have not been performed yet, initial studies suggest that like other cationic systems, they exhibit toxicity at high concentrations. When deciding to use a cell penetrating agent in a drug delivery system, the concentration used must not impart a toxic response in the host since drug delivery systems are not intended to be toxic.

1.19 Thesis goals

The goal of this thesis is to explore in more detail the effects of the dendritic surface functionalization on both the physical and biological properties of polymer vesicles. Vesicles based on PBD-PEO and PCL-PEO are studied and the dendrons investigated possess three

different peripheral functionalities - neutral hydroxyls, cationic primary amines and finally cationic guanidines. Unfunctionalized polymer vesicles are used as a control group. The effects of the dendrons on the release rates of molecules from the vesicles is investigated using rhodamine B as a model small molecule, while rhodamine B labeled bovine serum albumin (BSA) was investigated as a model biomacromolecule. This provides insight into the effects of the dendritic groups on the vesicle stability. The cytotoxicities of vesicles functionalized with the different dendritic groups are evaluated using the MTT assay. Finally, the effects of the peripheral functionalities of the dendritic groups on the internalization of the vesicles in HeLa cells are investigated by fluorescence confocal laser scanning microscopy.

Part Two: Results and Discussion

2.1 Synthesis

2.1.1 Synthesis of Dendrons

To test the effect of branched surface functionality on polymer vesicles, polyester dendrons based of 2,2-bis(hydroxymethyl)propionic acid were selected because of their ease of synthesis,[51] biocompatibility,[27] and the fact that this dendron has been used in our previous work.[48] All of the dendrons contained a focal point alkyne group designed to undergo a click reaction with an azide group of the vesicle periphery as in the group's previous work. This dendron was synthesized by a divergent method shown in Scheme 1, involving the reaction of alcohol groups on the dendron periphery with an anhydride derivative of the monomer containing acetonide protecting groups on alcohols. At the third generation, the hydroxyl groups on the periphery of dendron **1** were reacted with a β-alanine based anhydride (Scheme 2) to produce a dendron (**2**) with primary amines on the periphery after deprotection of the Boc groups.

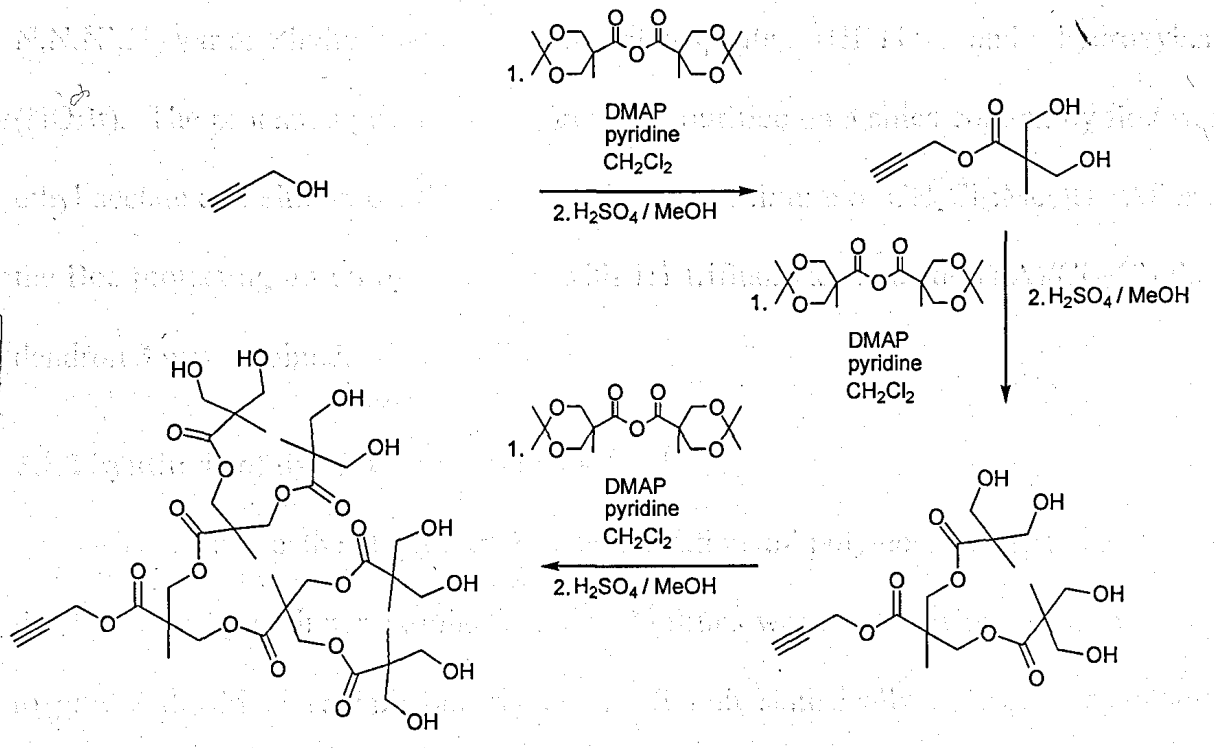

Scheme 1. Divergent synthesis of a third generation polyester dendron.

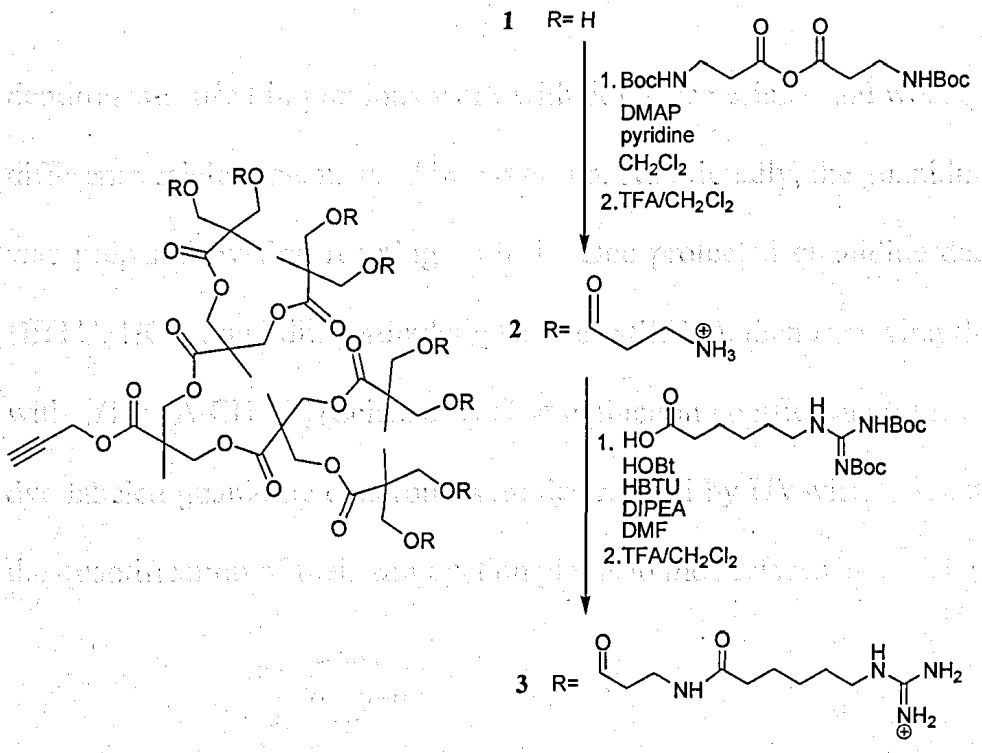

Scheme 2. Functionalization of a third generation dendron from hydroxyl functionality to amine and guanidine functionality.

From the deprotected amine dendron, guanidine functionality was installed on the periphery by reaction with N,N'-bis(BOC)-6-guanidinylcaproic acid, O-benzotriazole-N,N,N',N'-tetramethyluronium hexafluorophosphate (HBTU) and hydroxybenzotriazole (HOBt). The protected guanidine dendron was purified on a silica column by first washing with ethyl acetate and elution off the column with a 9:1 mixture of CH_2Cl_2:MeOH. After removal of the Boc protecting group by treatment with 1:1 trifluoroacetic acid (TFA)/CH_2Cl_2 the guanidine dendron **3** was obtained.

2.1.2 Synthesis of dye-labeled dendrons

To measure the degree of functionalization of polymer vesicles, the third generation dendron bearing peripheral amine functional groups was reacted with a rhodamine B derivative to give a dendron (**4**) with one rhodamine B unit statistically as previously reported.[34] This

dendron was used in previous work with polymer vesicles and would allow comparison between different vesicle systems used in our group. Additionally, the guanidine functionalized dendron **5** was prepared by first reacting with the Boc protected guanidine derivative in the presence of HBTU, HOBt, and diisopropylethylamine (DIPEA), then removing the Boc groups by treatment with 1/1 TFA/CH_2Cl_2 (Scheme 3). The extinction coefficients (ε) for the dye labeled amine and dye labeled guanidine dendrons were determined by UV-visible spectroscopy in order to enable the quantification of their conjugation yields to the surfaces of vesicles.

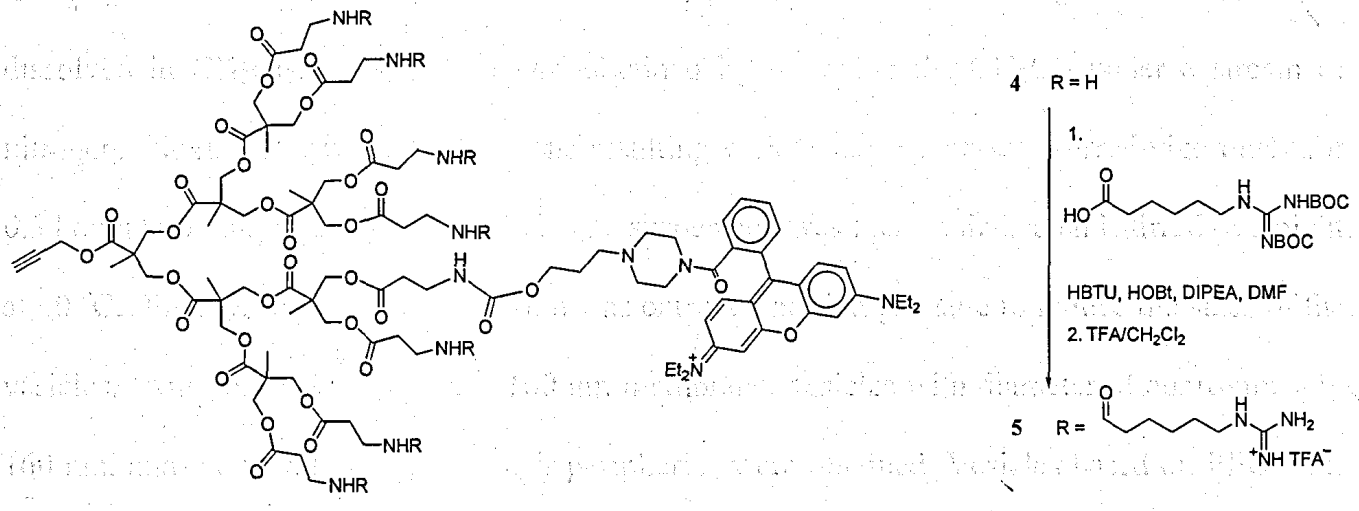

Scheme 3. Synthesis of Rhodamine labeled guanidine dendron.

2.1.3 Polymer Functionalization

Vesicles based on two different diblock copolymers were investigated in this work. One polymer was the amphiphilic linear diblock copolymer PBD–PEO with a composition of 6500 g/mol PBD (80% 1,2-addition) and 3900 g/mol PEO, **6**. Vesicles formed using closely related polymers have been extensively investigated and found to be highly stable and biocompatible.[22] A terminal azide group was introduced to PBD–PEO by reaction of the terminal hydroxyl with azidoacetic acid to provide PBD–PEO–N_3 (**7**).[34] The terminal azide, which should be presented on the vesicle surface, allows for the conjugation of a dendron with an alkyne focal point by a

copper (I) catalyzed 3 + 2 ''click'' cycloaddition.[34] The other polymers were PEO-PCL diblock copolymer, **8**, and the azide functionalized PEO-PCL, **9**, which were available from another member of the group.[27]

2.2 Vesicle Preparation

2.2.1 Vesicle Formation

Vesicles based on PBD-PEO were prepared using a thin film rehydration method. Commercially available PBD-PEO and azide-terminated PBD-PEO in a 4:1 mixture were dissolved in CH_2Cl_2. A thin film was obtained by removing the CH_2Cl_2 under a stream of nitrogen. Next, water was added and the resulting vesicle suspension was stirred vigorously for 0.5 hours to break up the polymer film. The suspension was then sonicated and stirred overnight at 40 °C. Finally, the vesicle suspension was extruded at high pressure to reduce the sizes of the vesicles. After extrusion through a 100 nm membrane, vesicles with diameter of approximately 160 nm, and with azide groups on their peripheries were obtained. Vesicles based on PEO-PCL with surface azide groups were prepared by the "solvent switch" method, as previously reported, by a member of the group, as seen in Figure 7.[27]

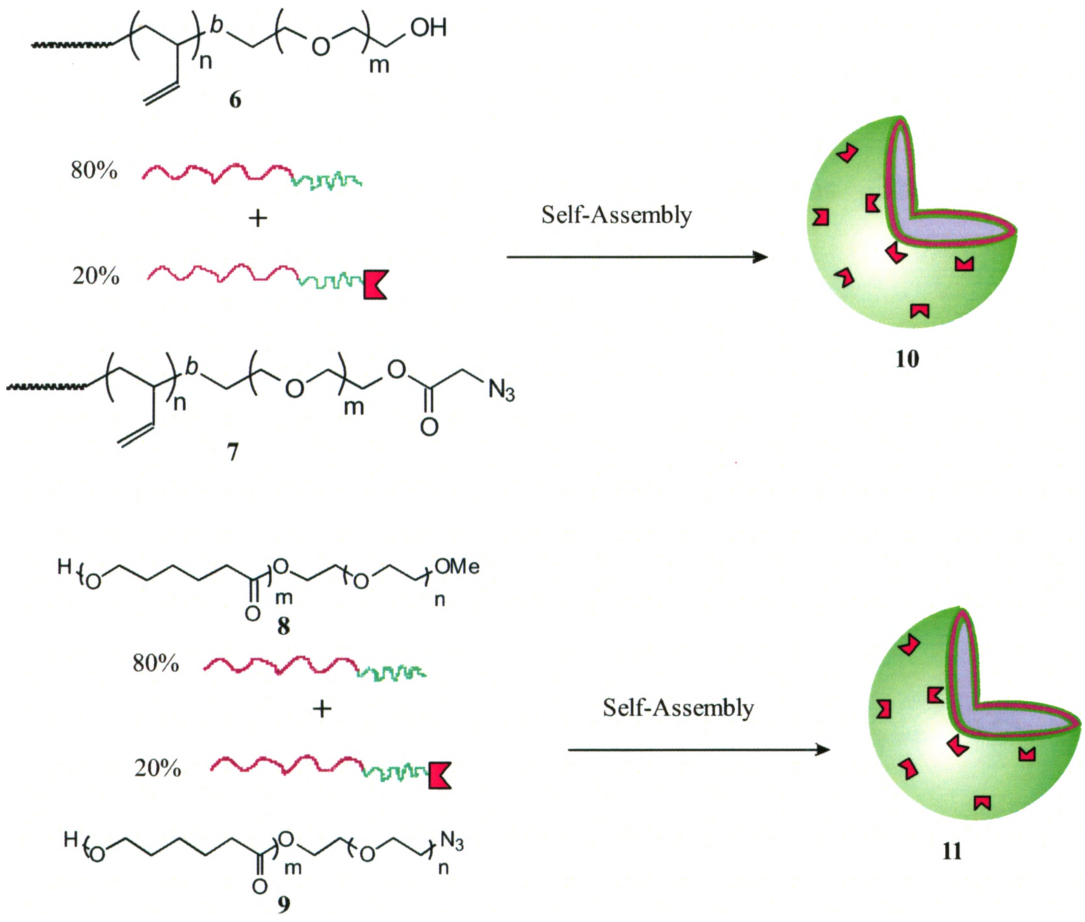

Figure 7. Self-Assembly of 20% azide functionalized PBD-PEO and PEO-PCL vesicles.

2.2.2 Surface Functionalization of Vesicles with Dendritic Groups

With the extruded vesicles in hand, different functionalized systems can be obtained by a click reaction using the procedure illustrated in Figure 16. Naked PBD-PEO vesicles, **10**, were used as a control group for the PBD-PEO vesicle system as they do not have any surface modification other than the terminal azide group. From vesicle sample **10**, the surface was modified to a neutral functionality by a reaction with **1** using click reaction conditions involving $CuCl_2$ and sodium ascorbate for 24 hours. The hydroxyl functionalized vesicles, **12**, were purified by dialysis in water. For cationic functionalized vesicles, vesicle sample **10** was mixed with **2** under click conditions. After 24 hours, amine functionalized vesicles, **13**, were purified by dialysis in water. The same procedure was used to produce guanidine functionalized vesicles

14. Another member of the group prepared vesicle sample **11** as previously reported.[27] From vesicle sample **11,** hydroxyl functionalized vesicles, **15**, were obtained by reaction with the hydroxyl functionalized dendron **1** under click conditions. The functionalized vesicles were purified by dialysis in water.

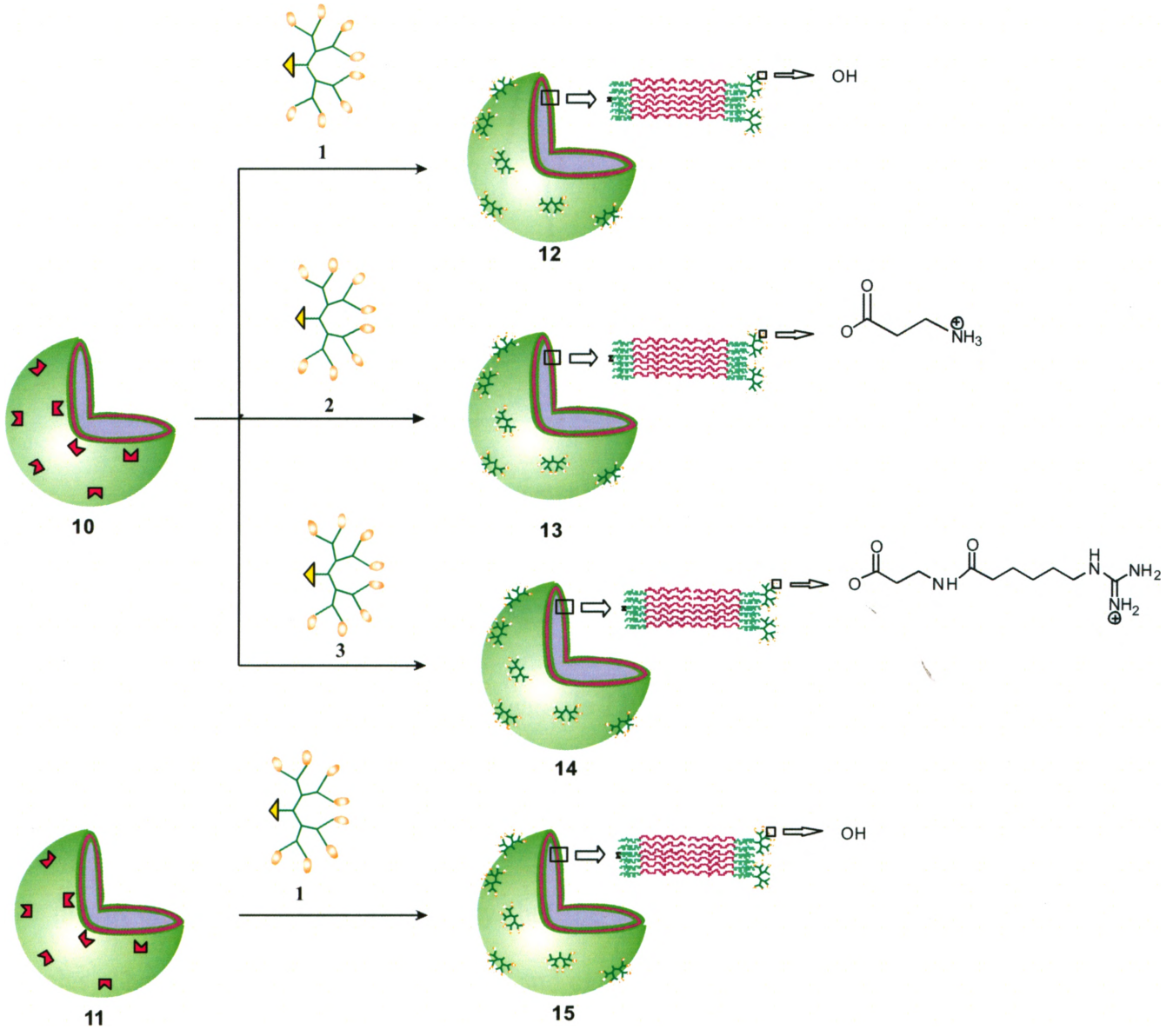

Scheme 3. Surface functionalization of polymer vesicles via click reaction.

The Z-average diameter of vesicle sample **10** was 160 nm with a polydispersity index (PDI) of 0.15, as shown in Figure 8. The bimodal size distribution indicates that there were two

different populations within the sample, the first being approximately 60 nm in diameter and the second being approximately 180 nm diameter. However, as the second population is three times the size as the first, it is possible that the second population is an aggregate of a few smaller vesicles.

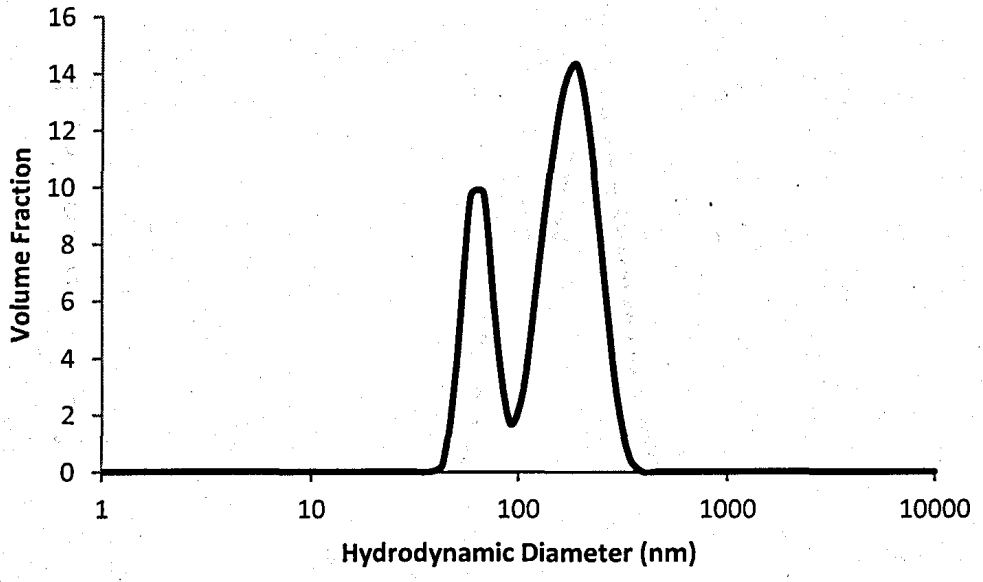

Figure 8. Size distribution of vesicle sample **10** expressed as a volume fraction.

The Z-average diameter of vesicle sample **12** was 170 nm with a pdi of 0.17, as shown in Figure 9. The bimodal distribution again indicates that there were 2 different populations within the sample, the first being approximately 75 nm in diameter and the second being approximately 220 nm in diameter. Again, it is likely that the larger population is aggregates of individual vesicles. The increased size of the vesicles and aggregates can be attributed to the addition of the dendrons, which may lead to a thicker vesicle membrane. The Z-average diameter of vesicle sample **13** was 180 nm with a PDI of 0.16, as seen in Figure 10. Again, a bimodal size distribution was obtained, likely due to aggregation, and the vesicles were larger than the unfunctionalized vesicles. The Z-average diameter of vesicle sample **14** is 200 nm with PDI of

0.24, as seen in Figure 11. Unlike with previous samples, vesicle sample **14** did not have a distinctively bimodal size distribution. However, the peak is not symmetric as there is a shoulder around 95 nm indicating this was likely just due to the inability of the instrument to resolve the two size populations.

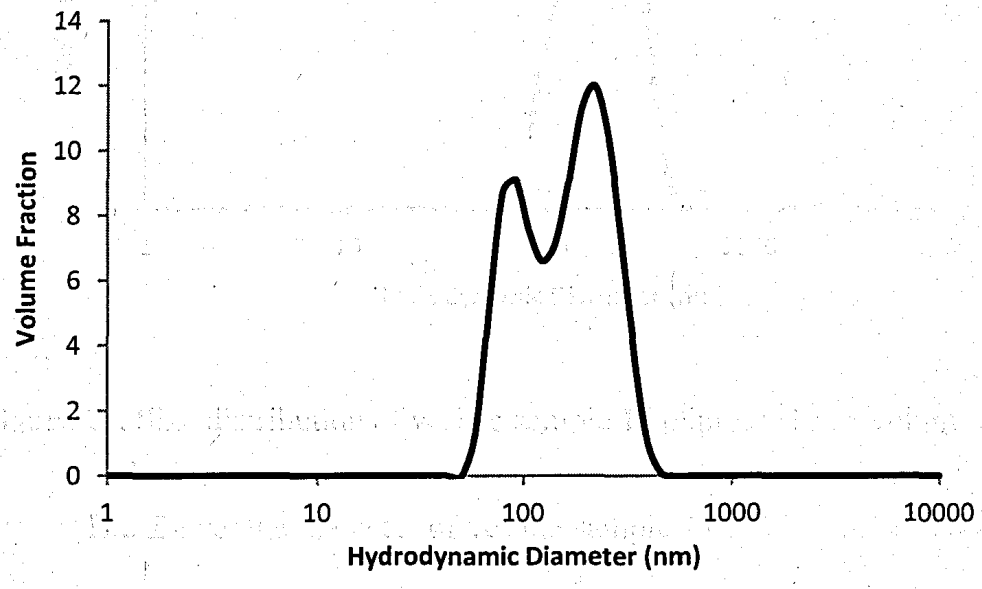

Figure 9. Size distribution of vesicle sample **12** expressed as a volume fraction.

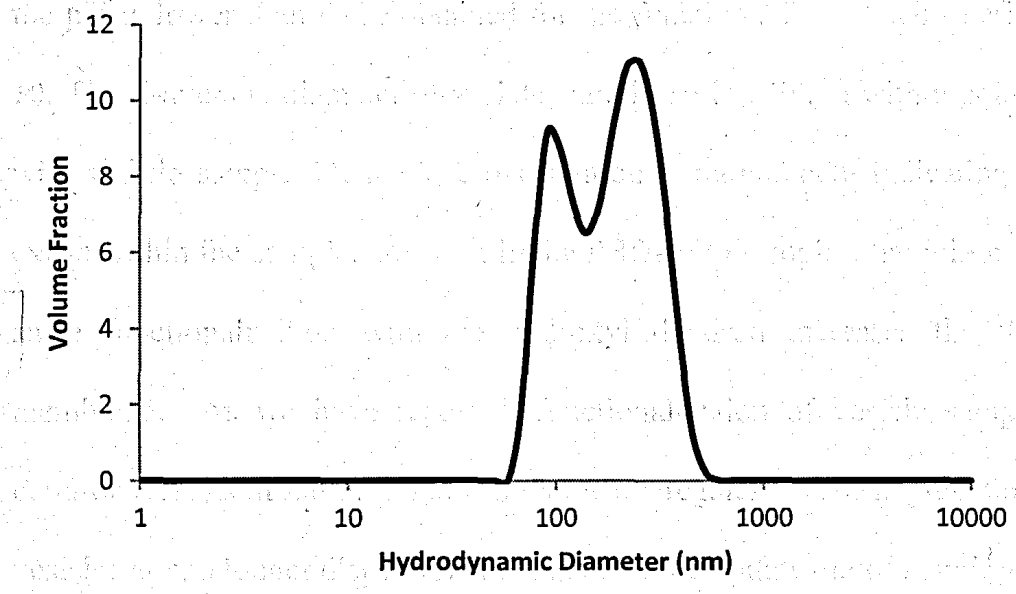

Figure 10. Size distribution of vesicle sample **13** expressed as a volume fraction.

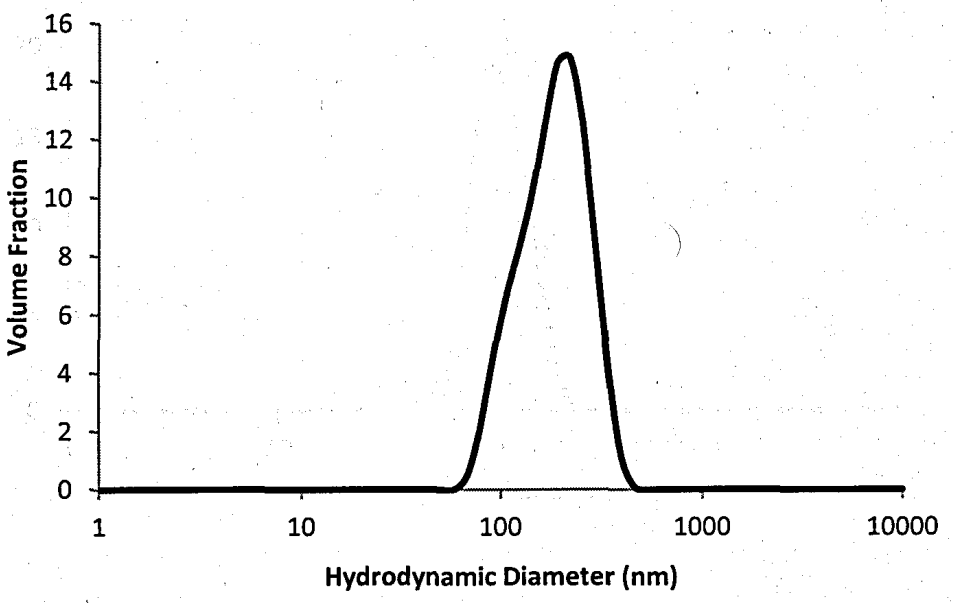

Figure 11. Size distribution of vesicle sample **14** expressed as a volume fraction.

The Z-average diameter of vesicle sample **11** is 120 nm with a PDI of 0.08, as shown in Figure 12. Unlike with the PBD-PEO samples, the peak is monomodal, indicating that a single population of particles exists in the sample. Furthermore, as the size distribution is monomodal, the pdi is lower than those obtained for the functionalized vesicles derived from vesicle sample **10**. The Z-average diameter of vesicle sample **15** is 140 nm with a pdi of 0.15, (Figure 13). As with vesicle sample **11**, the size distribution is monomodal indicating that a single population exists within the sample. As seen in the PBD-PEO samples, the minor size increase is expected since functionalization with the hydroxyl dendron increases the thickness of the vesicle membrane. As we have reported, functionalization of vesicle sample **11** with the cationic dendrons results in samples that form large aggregates.[27] The aggregation is so extensive that the vesicles are no longer dispersible in water and precipitate out of solution even at an azide loading below 20%. As a result, these samples were not tested further.

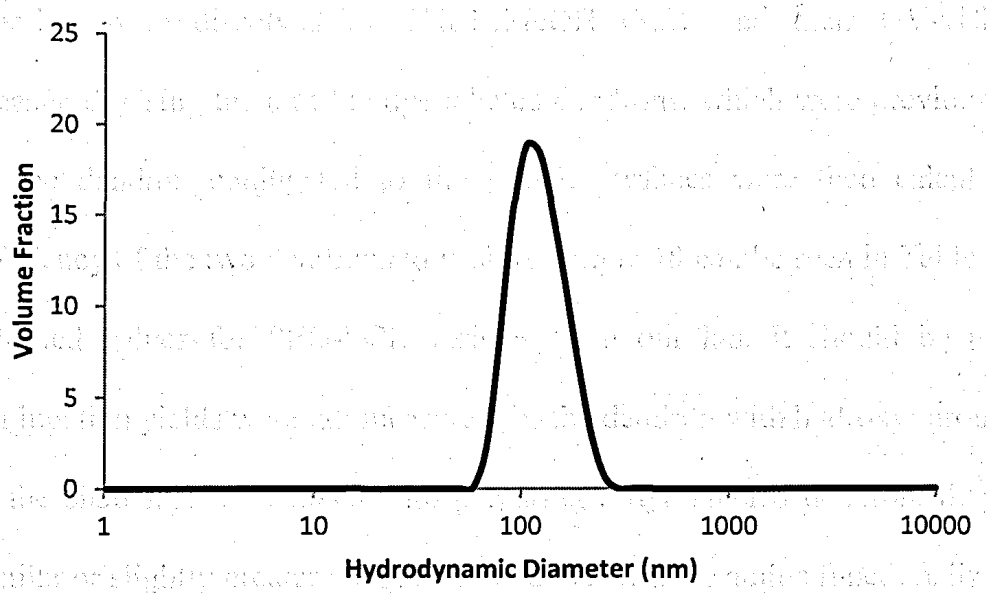

Figure 2. Size distribution of vesicle sample **11** expressed as a volume fraction.

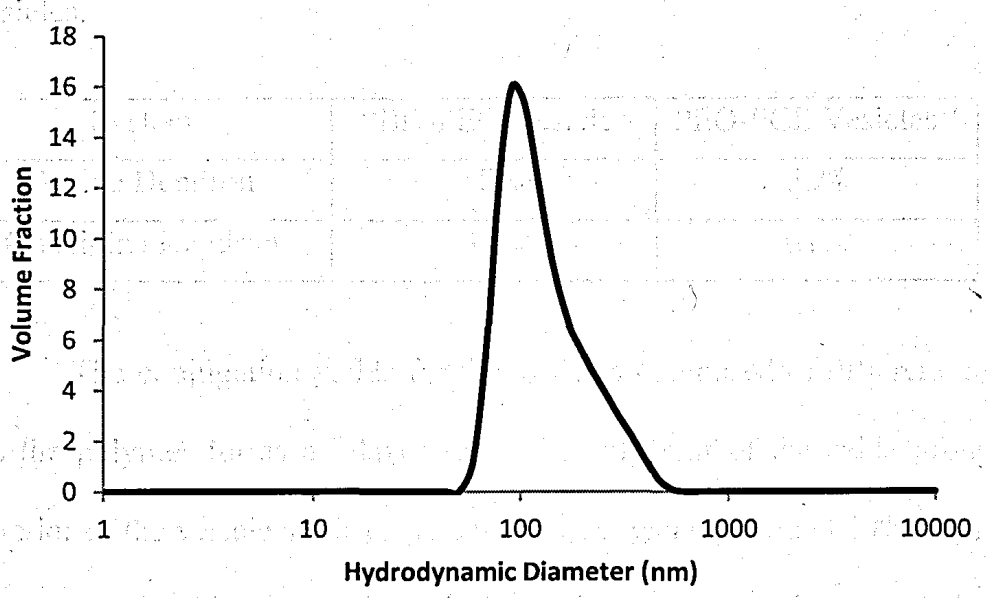

Figure 3. Size distribution of vesicle sample **15** expressed as a volume fraction.

2.2.3 Quantification of Dendron Conjugation

In order to quantify the degree of dendron conjugation, click reactions were performed as described above, but using the dye labeled dendrons **4**, and **5**. Following the removal of the excess dendron by dialysis and then evaporation of the water, the materials resulting from each

reaction were dissolved in $CHCl_3$:MeOH (3:2), and their UV-visible absorbances were measured. Using the ε of the dye labeled dendrons, which were previously measured, the yields of the dendron conjugated to the vesicle surfaces were then calculated. The conjugation efficiency of the two dendrons to vesicle sample **10** can be seen in Table 1 along with previously reported values for PEO-PCL vesicles from our lab. It should be noted that although the conjugation yields were not measured for the dendron with hydroxyl groups on the periphery due to the challenges associated with preparing a dye-labeled dendron, they can be inferred to be similar or slightly greater than those obtained with the amine functionalized dendron.

Table 1. Conjugation efficiency of amine and guanidine dendrons to the surface of polymer vesicles.

System	PBD-PEO Vesicles	PEO-PCL Vesicles[27]
Amine Dendron	48%	58%
Guanidine Dendron	37%	41%

The conjugation yields for the vesicles composed of different copolymers were similar. As the polymer forms a bilayer structure, only half of the azide groups are displayed on the exterior of the vesicle surface. The theoretical yield is around 50% as the dendron would not be expected to readily diffuse through the vesicle membrane because of its large size and cationic charge. However, as previously argued[34] the vesicle membrane is dynamic and individual polymer strands may flip orientation from the interior of the vesicle to the exterior of the vesicle. This characteristic of polymer vesicles would allow for yields greater than 50%, which are reported for lower azide loadings. Furthermore, the conjugation of dendron **5** has a lower yield for both the PBD-PEO and PEO-PCL systems. This is expected as the guanidine dendron is

larger than the amine dendron and sterics on the vesicle surface would inhibit conjugation of the dendron.

2.3 Encapsulation and Release of Small Molecules and Proteins

The study of the encapsulation and release of molecules from the dendron functionalized vesicles is of interest for several reasons. First, as destabilization or disruption of the vesicles would likely result in the release of encapsulated molecules, the release rates of these molecules may provide insight into how the introduction of the different dendrons to the vesicles surfaces affects the stability of the resulting vesicles. In addition, if these materials are to be used for drug delivery applications, it is important to gain insight into their release kinetics. In this work the release of both small molecules and macromolecules was investigated. Small molecules might be expected to diffuse across the vesicle membrane or be released upon vesicle disruption. Thus the release rate of small molecules would provide insight into vesicle stability as well as membrane permeability. On the other hand, macromolecules would not be expected to readily diffuse across the vesicle membrane and thus vesicles would likely have to be disrupted to release the molecules.

2.3.1 Encapsulation and Release of Rhodamine B

To measure the rate of release of encapsulated small hydrophilic molecules, a fluorescent rhodamine B was chosen as a model compound. It was selected as it is highly absorbant and fluorescent, thus enabling ready detection of its release. In order to encapsulate it, vesicles were formed as above but in a rhodamine B solution, the click reactions were performed to introduce the dendrons, the vesicles were extruded, and finally the nonencapsulated rhodamine B was removed by rapid dialysis using a Slide-a-lyzer dialysis cassette. In order to determine when the nonencapsulated dye had completely diffused across the dialysis membrane, a control dialysis

containing rhodamine B in the same concentration as used to form the vesicles was run at the same time as the vesicle solutions, and when the dye had left the cassette in the control group, the release experiment began. PEO-PCL vesicles were prepared as above except rhodamine B was dissolved in the water added to the copolymer during vesicle formation. The free rhodamine B was removed as in the PBD-PEO vesicle method. With the loaded vesicles in hand, the dialysis water was replaced with 0.1 M phosphate buffer water containing 0.01M sodium azide at 37°C. Every hour an aliquot was taken from the dialysate and its fluorescence was measured to determine the extent of release.

The release of encapsulated rhodamine B from vesicle sample **10** can be seen in Figure 14. The data was fit to a first order release model for a sphere with a polymeric exterior where percent release = $M_1 + M_2*(1-\exp(-M_3*t))$. In the equation, M_1 corresponds to percent release at time zero, M_2 corresponds to maximum release, M_3 is dependent on diffusivity of the dye through the polymer membrane, and t is time in hours. The first order release model was found to best fit the data in comparison to other models, and corresponds to encapsulated rhodamine B diffusing through the vesicle membrane. The M_1, M_2 and M_3 values of the curve fit can be seen in Table 2 along with R values and error. For vesicle sample **10**, a value of -5.4 was obtained for M_1, 100 for M_2 and 0.17 for M_3. Furthermore, the R value of the fit is 0.95, indicating that there is a good fit to the release profile. While none of the data points had a negative percent release value, allowing the M_1 values be less than zero a better fit to the data could be obtained. This could indicate that some nonencapsulated rhodamine B was still present within the dialysis cassette at t = 0. For vesicle sample **12** (Figure 15), a value of -0.057 was obtained for M_1, 85 for M_2 and 0.36 for M_3. As well, the R value of the fit is 0.93 indicating that there is a good fit to the release profile. The M_3 value is more than double the value obtained for vesicle sample **10**

suggesting that there is a change in the diffusivity of the dye. This suggests that the presence of the dendritic groups may destabilize the polymer bilayer to some extent, allowing the dye to more readily diffuse across the vesicle membrane." For vesicle sample **13** (Figure 16), a value of 2.3 was obtained for M_1, 83 for M_2 and 0.45 for M_3. As well, the R value of the fit is 0.94 indicating that there is a good fit to the release profile. In this case, the M_3 value is 0.45. This suggests that the dendron on the surface alters the diffusivity of the dye through the membrane. Furthermore, m_3 is larger than that of vesicle sample **12** which could be attributed to the positive charge of the dendron periphery which leads to some additional vesicle destabilization. For vesicle sample **14** (Figure 17), a value of 0.74 was obtained for M_1, 96 for M_2 and 0.34 for M_3. As well, the R value of the fit is 0.94 indicating that there is a good fit to the release profile. The presence of the guanidine functionality results in similar result as seen with vesicle sample **12** and vesicle sample **13** but the value for M_3 is similar to vesicle sample **12** and not vesicle sample **13** which disproves that the positive charge results in a greater diffusivity as compared to neutral functionality on the dendron periphery. Furthermore, it appears that the dendron architecture is responsible for the change in release rate relative to the unfunctionalized system and not the functionality on the periphery of the dendron. For vesicle sample **11** (Figure 18), a value of 6.9 was obtained for M_1, 86 for M_2 and 0.13 for M_3. As well, the R value of the fit is 0.94 indicating that there is a strong fit to the release profile. Interestingly, the mathematic model is the same for both the PBD-PEO systems and the PEO-PCL systems and the M_1, M_2 and M_3 values are similar to vesicle sample **10**. This indicates that the hydrophobic block composition does not change the mechanism of release of encapsulated small molecules.

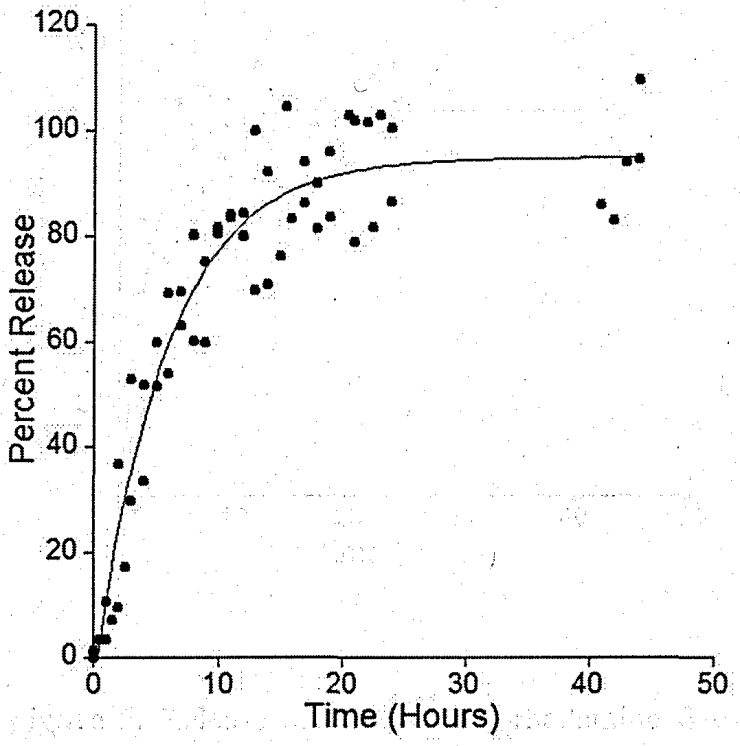

Figure 4. Release of encapsulated rhodamine B expressed as percent released from vesicle sample **10**. The data was fit to a first-order model.

Table 2. Coefficients of curve-fit from Kaleida Graph 4.0 for a first-order model.

Sample #	M_1	M_2	M_3	R value
10	-5.4 ± 4.3	100 ± 4.3	0.17 ± 0.02	0.96
12	-0.057 ± 5.1	85 ± 5.1	0.36 ± 0.04	0.93
13	2.3 ± 4.7	83 ± 4.7	0.46 ± 0.05	0.94
14	0.74 ± 4.8	96 ± 4.8	0.34 ± 0.04	0.94
11	6.9 ± 4.6	84 ± 5.7	0.13 ± 0.02	0.95

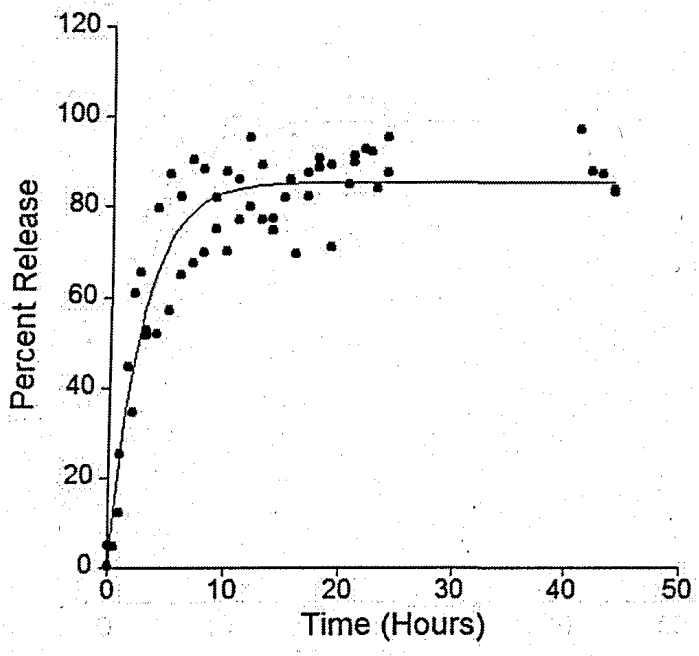

Figure 5. Release of encapsulated rhodamine B expressed as percent released from vesicle sample **12**. The data was fit to a first-order model.

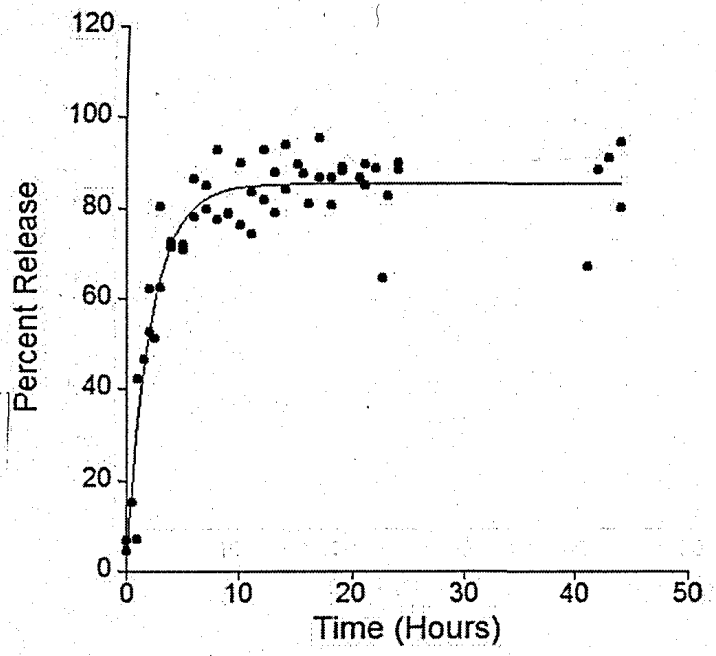

Figure 6. Release of encapsulated rhodamine B expressed as percent released from vesicle sample **13**. The data was fit to a first-order model.

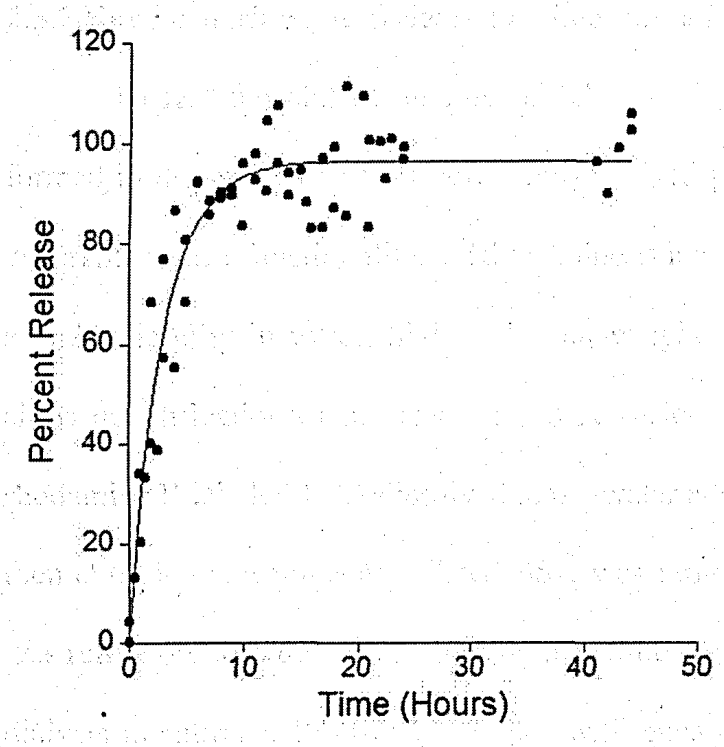

Figure 7. Release of encapsulated rhodamine B expressed as percent released from vesicle sample **14**. The data was fit to a first-order model.

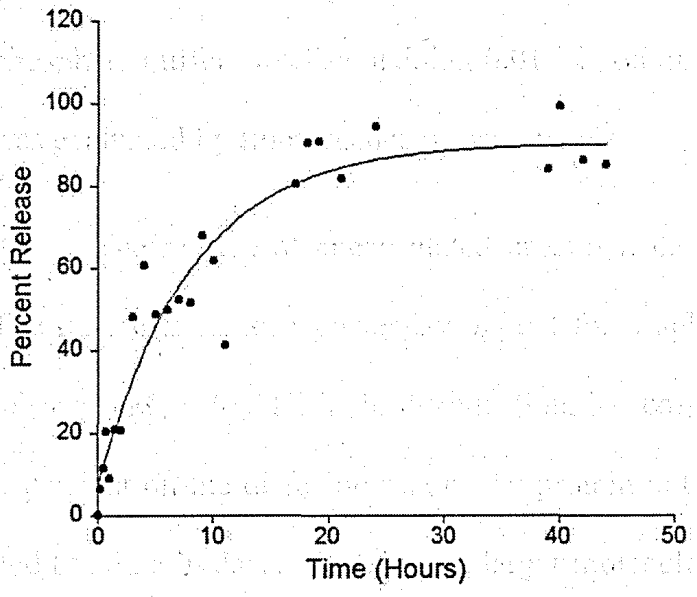

Figure 8. Release of encapsulated rhodamine B expressed as percent released from vesicle sample **11**. The data was fit to a first-order model.

2.3.2 Encapsulation and Release of Rhodamine labeled BSA

To test the change in rate of release of encapsulated macromolecules, vesicles were formed in the presence of a fluorescently labeled protein, followed by click reactions installing different surface functionalities. Rhodamine B labeled BSA was selected as a model since it has a high solubility in water, high molecular weight, and its fluorescence properties would easily allow quantification of its release rate. A vesicle solution was prepared as above except with rhodamine B labeled BSA dissolved in the water added to the thin film. The vesicle solution was then extruded and nonencapsulated BSA was removed by dialysis. Again a control experiment was run in order to determine the length of time required for the free protein to diffuse across the dialysis membrane. PEO-PCL vesicles with encapsulated protein were prepared by dissolving the protein in the water that was added to the dissolved copolymer during vesicle formation. The non-encapsulated protein was removed in the same manner as for the PBD-PEO vesicles.

With the protein-loaded vesicles in hand, the dialysis water was replaced with 0.1 M phosphate buffer water containing 0.01 M sodium azide at 37 °C. Each day the protein release was evaluated by fluorescence measurements.

The release of encapsulated protein from vesicle sample **10** can be seen in Figure 19. The data was fit to a power-law model for a sphere with a polymeric exterior where percent release = $M_4 + M_5*t\text{^}M_6$. In the equation, M_4 corresponds to percent release at time zero, M_5 is dependent on the diffusion rate of the protein out of the vesicle, M_6 is the diffusion coefficient and t is time in days. Proteins are larger molecules and would have difficulty diffusing through the hydrophobic region of the polymer membrane which suggests a different mechanism of release for encapsulated proteins. The power-law model corresponds to encapsulated rhodamine labeled BSA diffusing through temporary pores which form in the vesicle membrane. The

protein still diffuses down its concentration gradient. The M_4, M_5 and M_6 values of the curve fit can be seen in Table 3 along with R values and error. This equation can only be used to model the initial phase of the release; as t approaches ∞, percent release would also approach ∞. However percent release cannot exceed 100% and as a result, another mathematic model is needed to describe release approaching 100% release. This was not an issue in these experiments because none of the samples reached 100% release. As with small molecule release, none of the data points had a negative percent release value however by allowing M_4 be less than zero, a stronger fit to the data could be obtained. For vesicle sample **10**, a value of 2.8 was obtained for M_4, 33 for M_5 and 0.35 for M_6. Furthermore, the R value of the fit is 0.95, indicating that there is a good fit to the release profile. For vesicle sample **12** (Figure 20), a value of -0.63 was obtained for M_4, 52 for M_5 and 0.24 for M_6. As well, the R value of the fit is 0.97 indicating that there is a good fit to the release profile. The M_6 value is less than the value obtained for vesicle sample **10** suggesting that there is a change in the diffusivity of the protein. For vesicle sample **13** (Figure 21), a value of 0.70 was obtained for M_4, 25 for M_5 and 0.44 for M_6. As well, the R value of the fit is 0.97 indicating that there is a good fit to the release profile. In this case, the M_6 value is 0.44. This suggests that the dendron on the surface alters the diffusivity of the dye through the membrane. Furthermore, M_6 is larger than that of vesicle sample **12**, which could be attributed to the positive charge of the dendron periphery that leads to some additional vesicle destabilization. For vesicle sample **14** (Figure 22), a value of 4.0 was obtained for M_4, 22 for M_5 and 0.48 for M_6. As well, the R value of the fit is 0.95 indicating that there is a good fit to the release profile. The presence of the guanidine functionality results in a similar result as seen with vesicle sample **13** suggesting the positive charge results in a greater diffusivity as compared to neutral functionality on the dendron periphery. For vesicle sample **11**

(Figure 23), a value of 2.9 was obtained for M_4, 33 for M_5 and 0.34 for M_6. As well, the R value of the fit is 0.96 indicating that there is a strong fit to the release profile. As with encapsulated small molecules, the mathematic model is the same for both the PBD-PEO systems and the PEO-PCL systems and the M_4, M_5 and M_6 values are similar to vesicle sample **10**. This indicates that the hydrophobic block composition does not change the mechanism of release of encapsulated proteins.

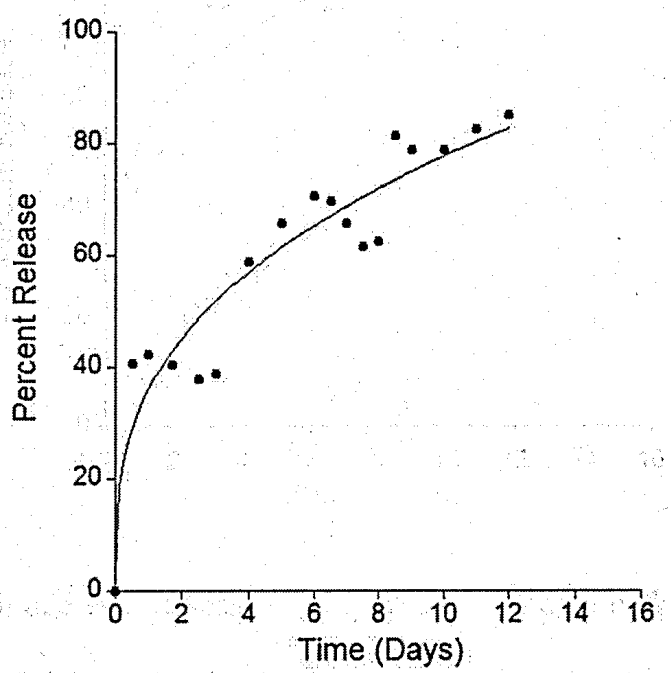

Figure 99. Release of encapsulated rhodamine labeled BSA expressed as percent released from vesicle sample **10**. The data was fit to a power-law model.

Table 3. Coefficients of curve-fit from Kaleida Graph 4.0 for a power law model.

Sample #	M_4	M_5	M_6	R value
10	2.8 ± 7.2	33 ± 7.6	0.35 ± 0.07	0.95
12	-0.63 ± 5.8	52 ± 6.4	0.24 ± 0.04	0.97

13	0.70 ± 5.0	25 ± 5.0	0.44 ± 0.07	0.97
14	4.0 ± 6.9	22 ± 6.8	0.48 ± 0.10	0.95
11	2.9 ± 6.1	33 ± 6.2	0.34 ± 0.05	0.96

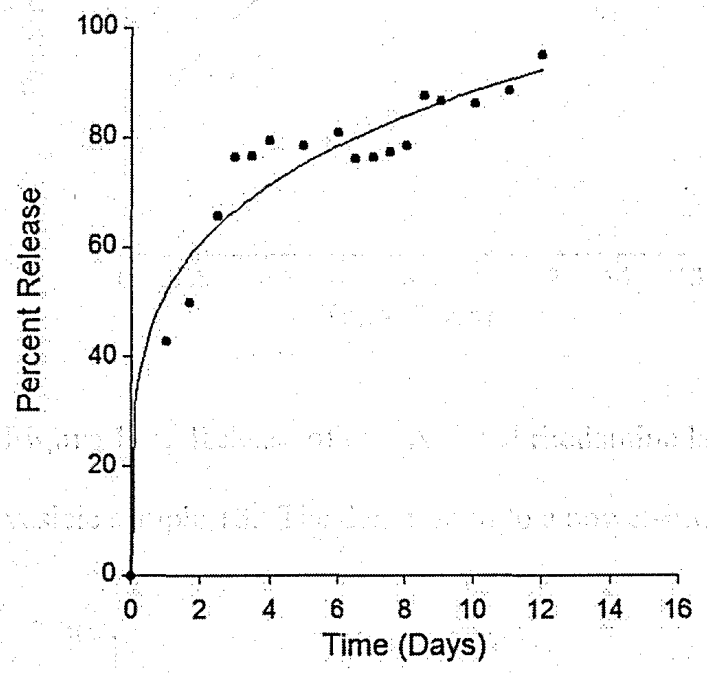

Figure 10. Release of encapsulated rhodamine labeled BSA expressed as percent released from vesicle sample **12.** The data was fit to a power-law model.

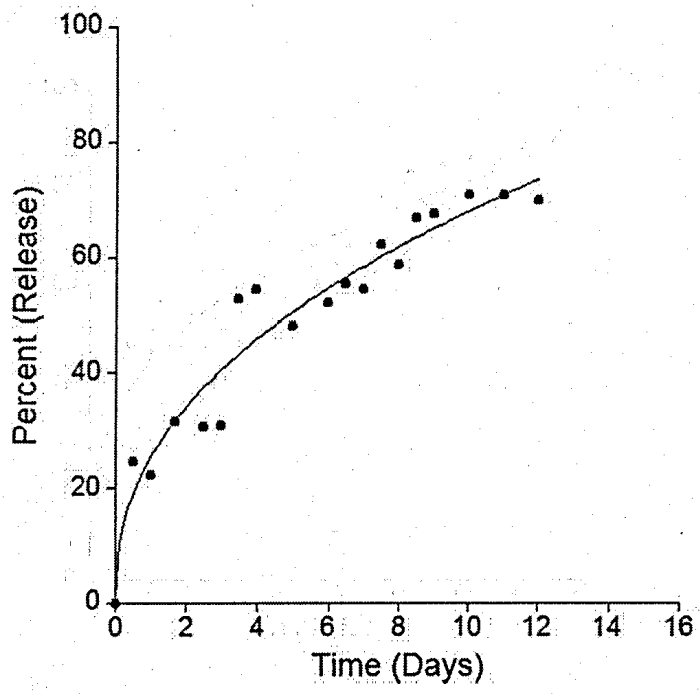

Figure 111. Release of encapsulated rhodamine labeled BSA expressed as percent released from vesicle sample **13**. The data was fit to a power-law model.

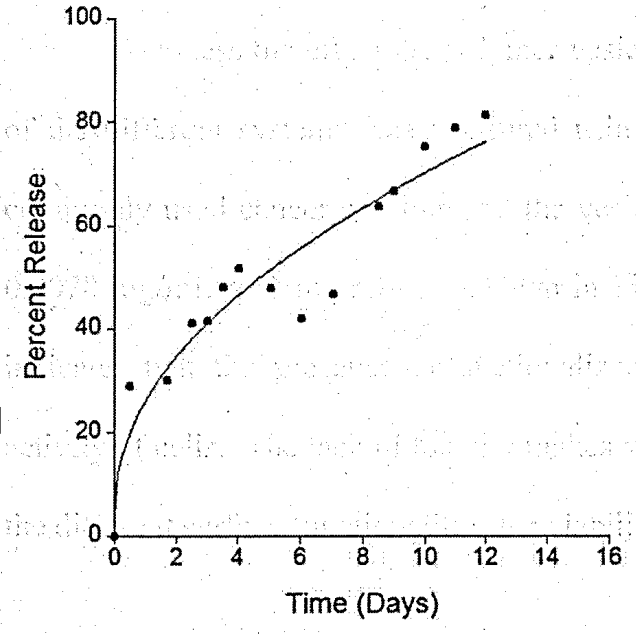

Figure 12. Release of encapsulated rhodamine labeled BSA expressed as percent released from vesicle sample **14**. The data was fit to a power-law model.

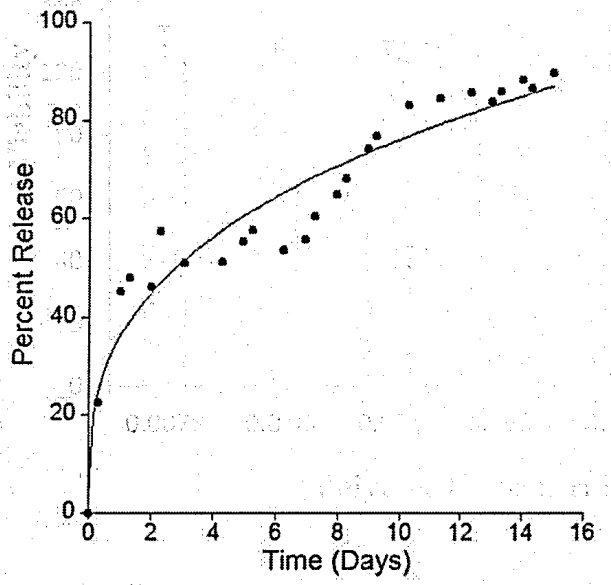

Figure 13. Release of encapsulated rhodamine labeled BSA expressed as percent released from vesicle sample **11**. The data was fit to a power-law model.

2.4 Cell Viability

To assess the effect the polymer vesicles had on the viability of cells, the toxicity profile of the different systems was measured using the MTT assay. HeLa cells were selected as a commonly used cancer cell line and the vesicles were evaluated at concentrations ranging from 0.0078 mg/mL to 1 mg/mL As shown in Figure 24, the toxicity profile for vesicle sample **10** indicates that the presence unfunctionalized polymer vesicles does not affect the metabolic activity of cells. The lack of toxicity makes vesicle sample **10** a good reference point to compare the different surface functionalities for viability.

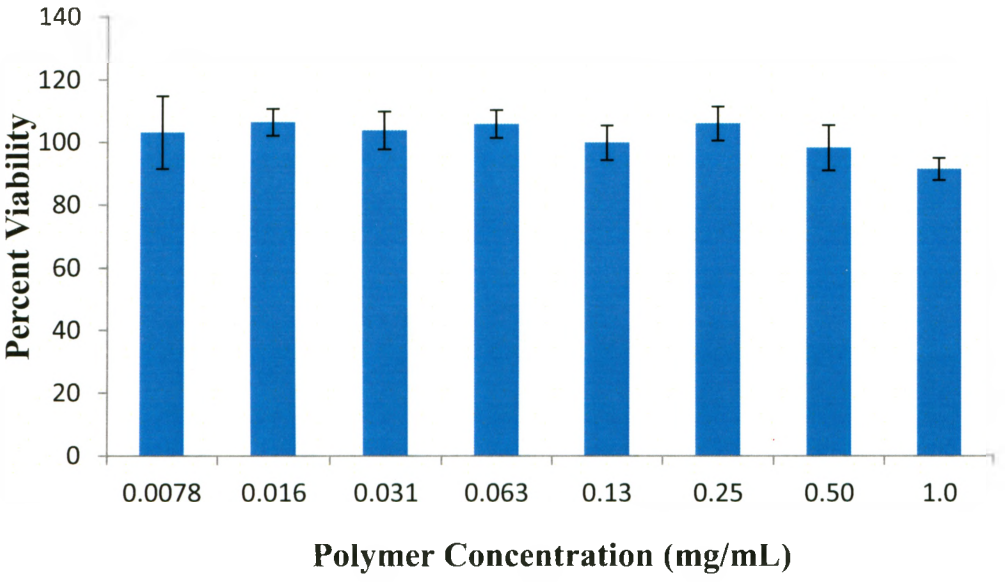

Figure 14. Toxicity profile of vesicle sample **10** as measured by the MTT assay. Error bars represent 1 standard deviation from the mean.

The toxicity profile for vesicle sample **12** is shown in Figure 25. The neutral hydroxyl functionality does not impart a toxic response at any of the concentrations tested, as the cell viability remains the same as that of control cells not exposed to vesicles. As shown in Figure 26, the amine functionality on the vesicle surface of vesicle sample **13** begins to induce toxicity at the highest concentrations tested, likely due to its cationic charge.[52] The toxicity profile for vesicle sample **14** is shown in Figure 27. At lower concentrations, the guanidine functionality does not affect the metabolic activity of cells. At the highest concentration, metabolic activity is below 60%. Its toxicity is greater than that of the amine functionality, indicating that cationic charge is not the only factor resulting in the toxic effect. This result is consistent with previous work since it has been reported that dendritic guanidine functionality imparts greater toxicity than primary amine functionality.[52,53] Nevertheless, at low concentrations, the guanidine

functionalized vesicles did not exhibit toxicity, indicating that they can still potentially be used to transport molecules into living cells.

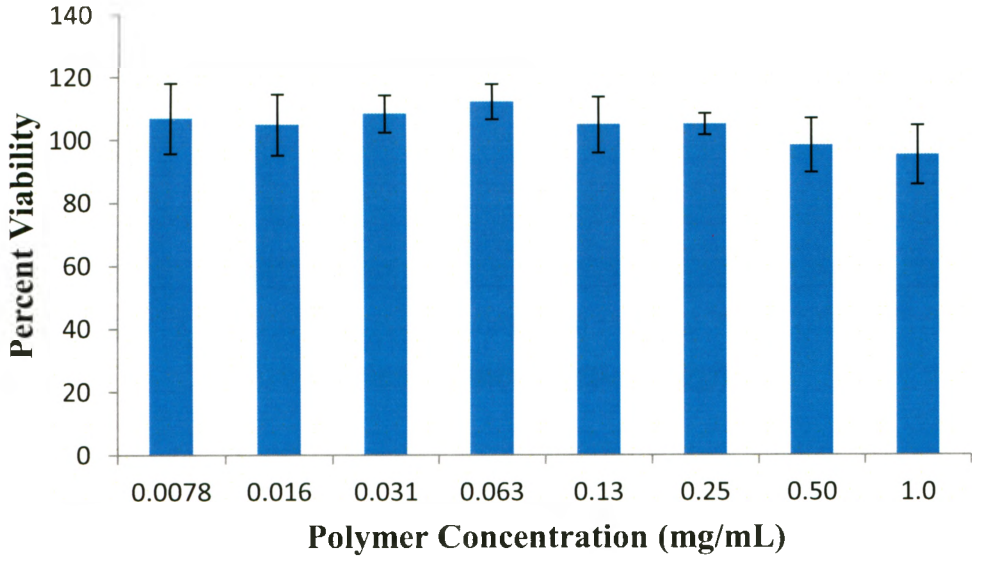

Figure 15. Toxicity profile of vesicle sample **12** as measured by the MTT assay. Error bars represent 1 standard deviation from the mean.

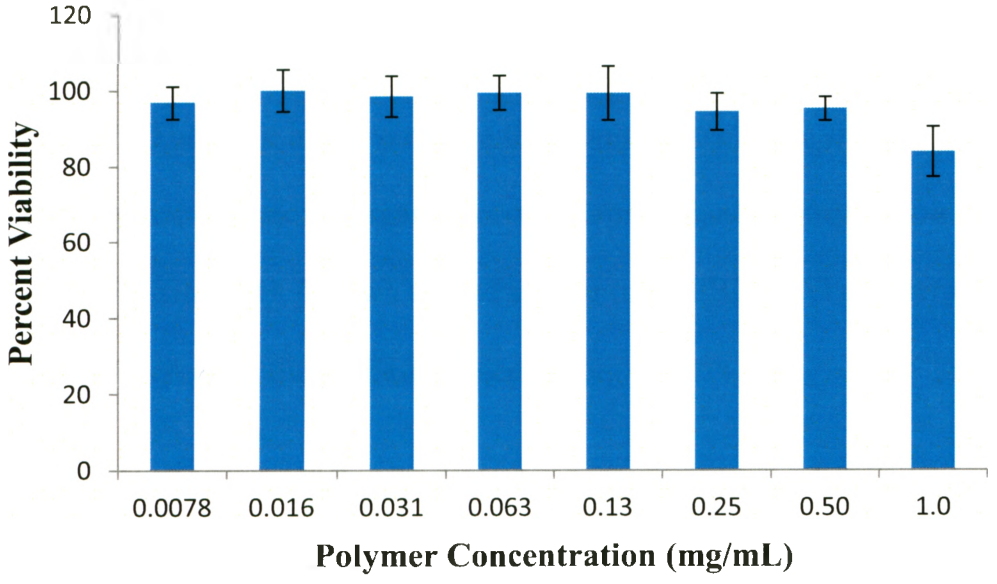

Figure 16. Toxicity profile vesicle sample **13** as measured by the MTT assay. Error bars represent 1 standard deviation from the mean.

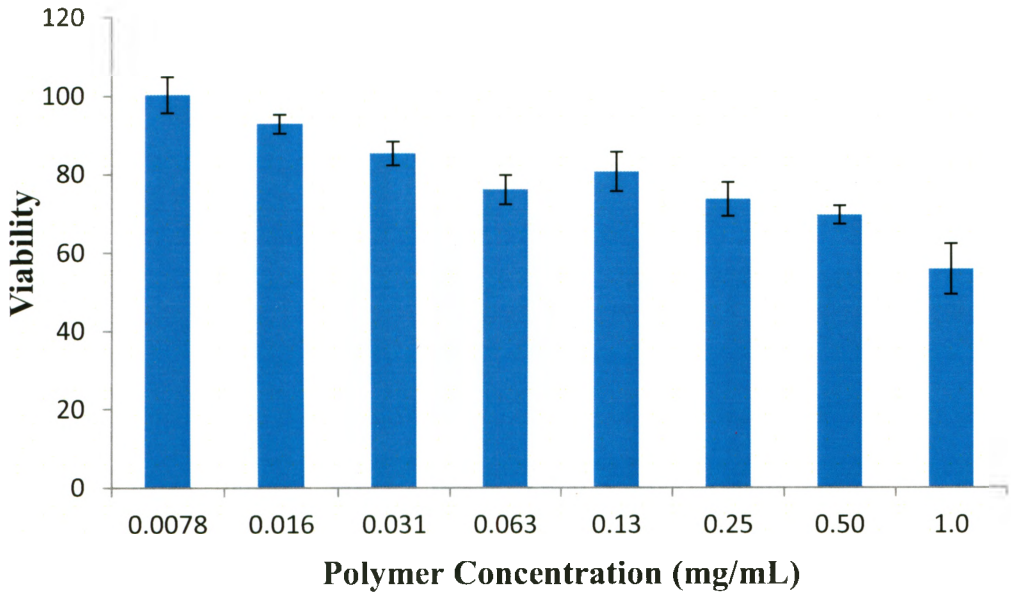

Figure 17. Toxicity profile of vesicle sample **14** as measured by the MTT assay. Error bars represent 1 standard deviation from the mean.

The toxicity profile of the PEO-PCL systems **11** and **15** is shown in Figure 28. The unfunctionalized vesicles **11** appear to be toxic as visibly lower viability values are observed relative to the PBD-PEO system and to vesicle sample **15**. While this trend is not expected since PCL-PEO is generally considered to be biocompatible, it was obtained on repeated attempts at this assay. There are many variables that could cause lower viability such as contamination in the copolymer or residual organic solvent remaining after purification. Unlike vesicle sample **11**, vesicle sample **15** follows a trend similar to its PBD-PEO counterpart except with some toxicity observed at the highest concentration.

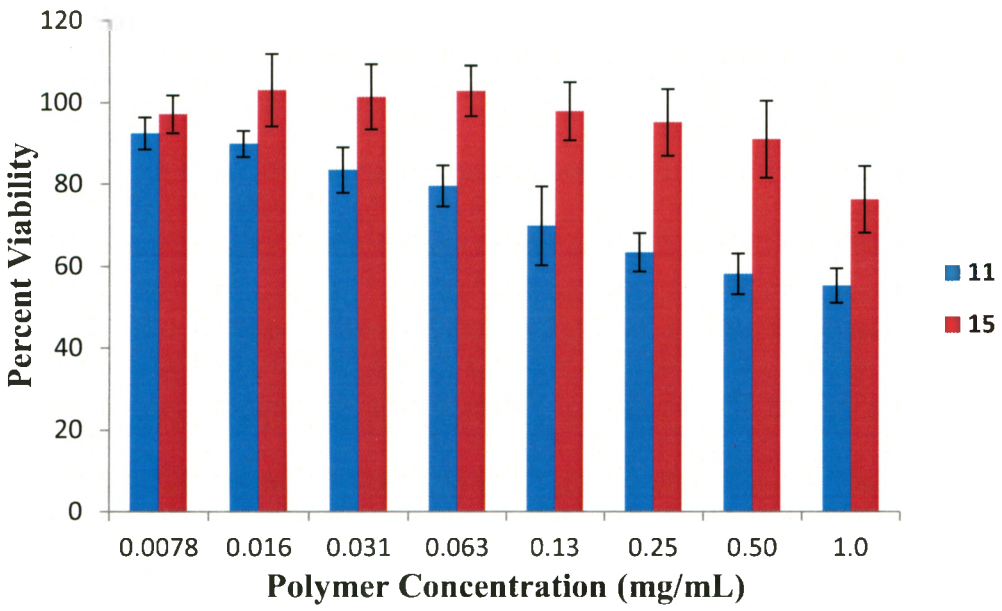

Figure 18. Toxicity profile of vesicle sample **11** and vesicle sample **15** as measured by the MTT assay. Error bars represent 1 standard deviation from the mean.

2.5 Cell Uptake

While it has been previously shown that nanoparticles that have been functionalized with dendrons do enter cells,[51] a comprehensive investigation has not been completed and the effects of the dendritic groups on the cell uptake of PBD-PEO or PEO-PCL vesicles have not yet been studied. To measure the cell internalization of the different systems, functionalized vesicle systems were prepared as above except containing 1% rhodamine B functionalized copolymer to allow visualization of the vesicles using fluorescence microscopy. Furthermore, since fluorescence is quantitative, this allows for the quantification of the amount of polymer within the cells. HeLa cells were used in these studies and the cell uptake of the different vesicles was examined both qualitatively and quantitatively following 1 hour incubations at 37 °C. The cell nuclei were stained with DAPI.[54]

As shown in Figure 29, after 1 hour incubation at 37 °C, in each case, the fluorescence did not appear to be specifically located in the nuclei but rather throughout the cytoplasm. Its somewhat punctate nature suggests that the polymers may be located within endosomal or lysosomal compartments, but further staining experiments are required to confirm this. The intensity of the fluorescence in the images corresponds to the amount of material in each since the images were captured under the same conditions and the concentration of dye remained constant throughout the experiment. While vesicle samples **10, 12** and **13** appear to have similar intensity, vesicle sample **14** appears to contain more polymer material, likely due to the guanidine group on the periphery since a similar result is not seen in vesicle sample **13**.

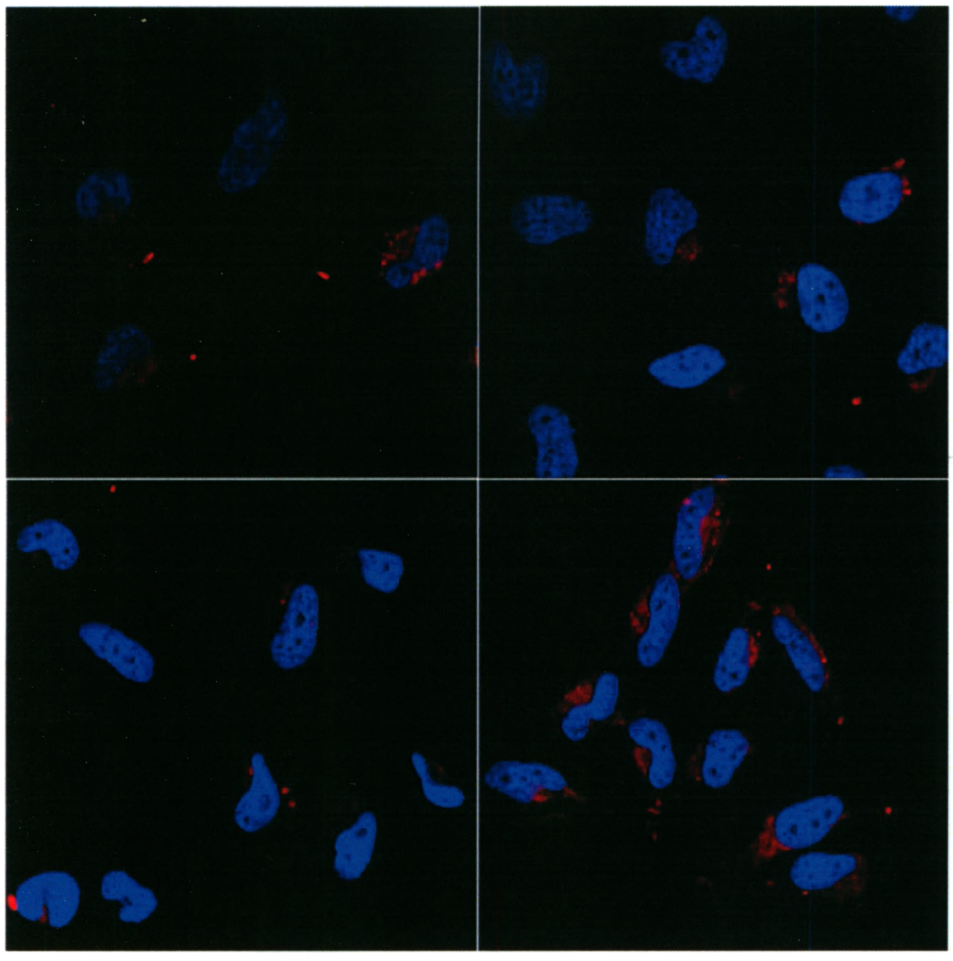

Figure 19. Confocal Microscope image of HeLa cells incubated with vesicle samples **10** (top left), **12** (top right), **13** (bottom left) and **14** (bottom right) at a concentration of 0.25 mg/mL with 1% rhodamine B dye labeled polymer. DAPI is seen in blue and rhodamine in red.

To obtain a quantitative result, the captured images were analyzed in Imagepro to measure the fluorescence intensities. The average relative intensity per cell for each sample can be seen in Figure 30. Vesicle samples **10**, **12**, **13** and **14** did exhibit statistically significant differences in fluorescent intensities as determined by a one way ANOVA test. However with further analysis using Post Hoc Tukey's Honestly Significant Difference (HSD) test and Scheffe's method, no significant difference was found between **10**, **12** and **13**. For Tukey's HSD, p-values obtained for vesicle samples **10** and **12**, **10** and **13**, and **12** and **13** were 0.53, 0.18

and 0.89 respectively. For Scheffe's method p-values of 0.61, 0.25 and 0.91 respectively were obtained. In contrast, consistent with the visibly greater fluorescence in Figure 28, vesicle sample **14** did have significantly greater uptake confirmed by Tukey's HSD and Scheffe's method because a p-value of less than 0.001 was obtained for each comparison. Thus, the presence of guanidine functionalities does seem to specifically enhance cell uptake, a result that was not obtained for vesicles functionalized with the dendron having cationic amine groups.

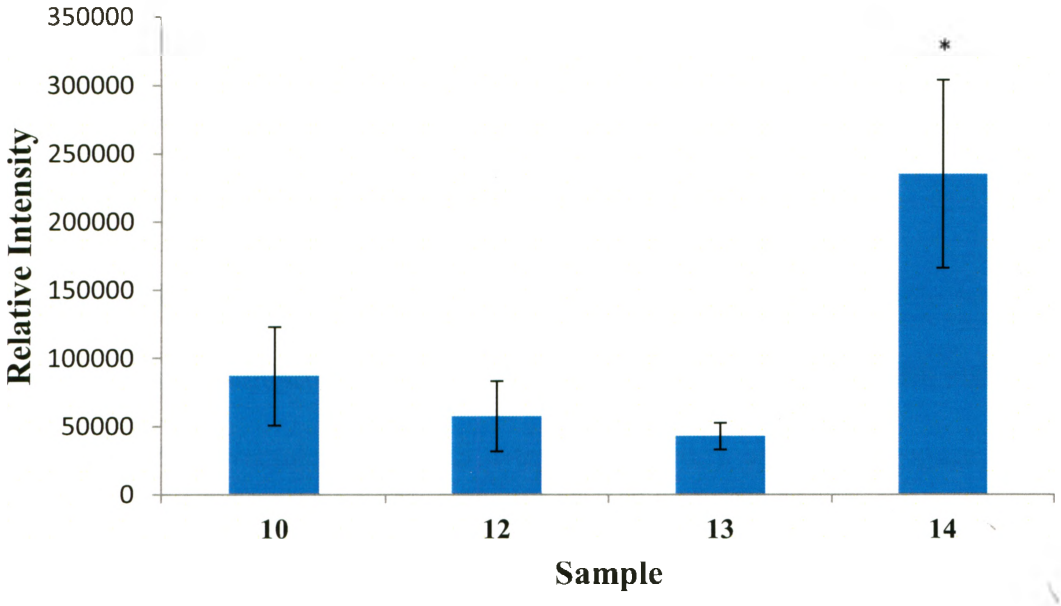

Figure 20. Intensity analysis of vesicle samples **10**, **12**, **13** and **14**. Error bars represent one standard deviation from the mean.

The internalized vesicle samples **11** and **15** as seen in Figure 31, similar to PBD-PEO vesicles at 37°C appear to be punctate throughout the cytoplasm of the cell. The PCL-PEO systems had aggregation issues, larger aggregates not internalized by cells were excluded from the counting algorithm as well as possible.

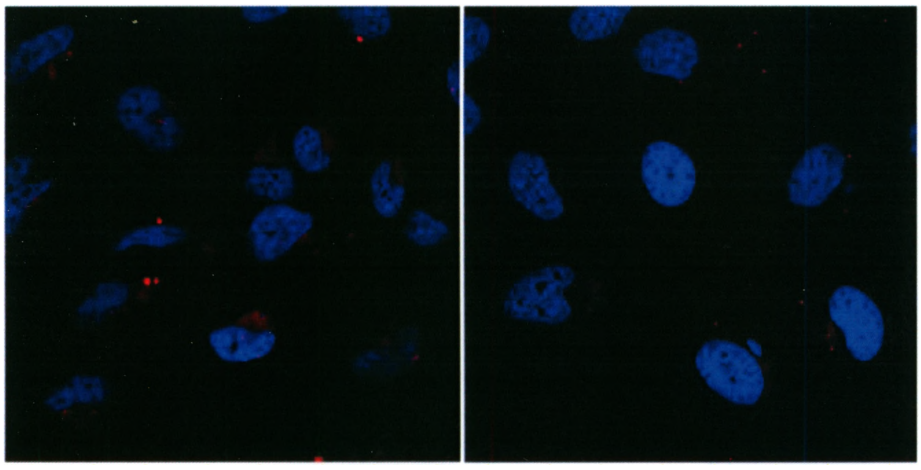

Figure 21. Confocal Microscope image of HeLa cells incubated with vesicle samples **11** (left) and **15** (right) at a concentration of 0.25 mg/mL with 1% rhodamine B dye labeled polymer. DAPI is seen in blue and rhodamine in red.

As with the PBD-PEO samples, captured images of vesicle samples **11** and **15** were analyzed using Imagepro. Interestingly, vesicle sample **11** did exhibit significantly increased cell uptake relative to vesicle sample **15** (t-test, $p < 0.005$), as seen in Figure 32, this could be due to aggregation issues of vesicle sample **15** since aggregated samples would be less likely to enter cells because of their larger diameter.

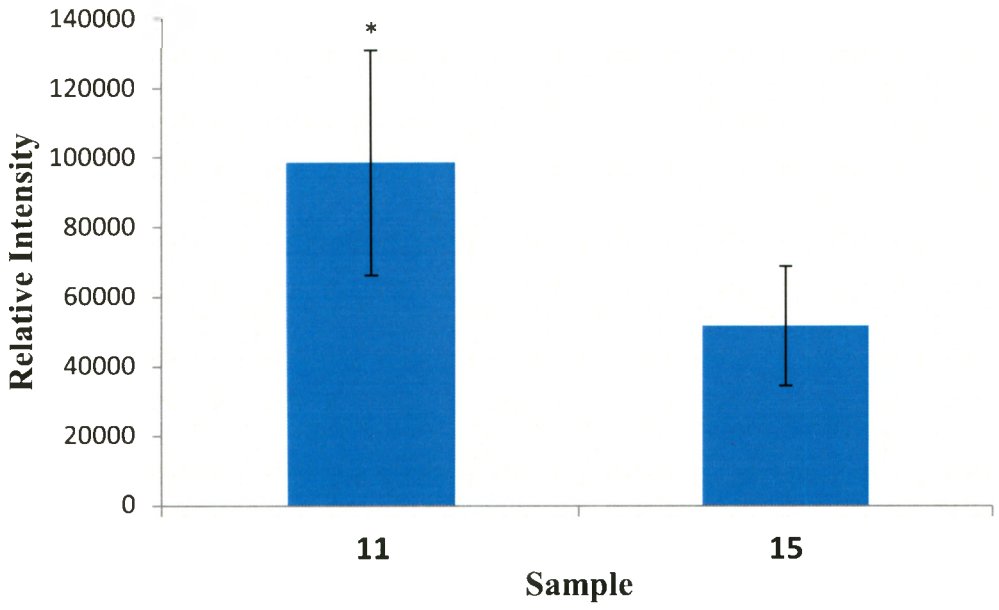

Figure 22. Intensity analysis of vesicle samples **11** and **15**.

Part Three: Conclusion

3.1 Conclusion

Polymer vesicles based on PBD-PEO and PCL-PEO were studied and dendrons possessing three different peripheral functionalities - neutral hydroxyls, cationic primary amines and finally cationic guanidines were investigated. The conjugation efficiencies of the cationic dendrons to the PBD-PEO vesicle surfaces were measured and the efficiencies were found to be similar to those of the previously reported reactions onto the surface of PEO-PCL vesicles. Next, the effects of the dendrons on the release of encapsulated small molecules from the vesicles was investigated using free rhodamine B as a model small molecule. The presence of the dendron architecture is likely responsible for the increase in release rate since all three functionalized systems had a similar rate increases. As well, the release rates were measured for encapsulated proteins. Unlike with the encapsulated small molecule, the functionality of the dendron does effect the release rate since the amine and guanidine both exhibited a quicker release profile. This suggests that the cationic charge could destabilize the vesicle structure. Next, the cytotoxicities of vesicles functionalized with the different dendritic groups were evaluated using the MTT assay. Cationic functionalities, more evident in the guanidine sample, produced a toxic response at higher concentrations but not at lower concentrations. Finally, the effects of the peripheral functionalities of the dendritic groups on the internalization of the vesicles in HeLa cells was measured by fluorescence confocal laser scanning microscopy. It was found that the guanidine functionalized vesicles resulted in increased internalization as compared to the other dendrons and control group. The images were analyzed using Imagepro software to quantify the relative degrees of internalization. It was found that the guanidine sample was statistically higher than the control group indicating that guanidine dendron does increase the cell

uptake of vesicles. This suggests that these materials may be useful for the transport of cargo into living cells.

Part Four: Experimental

4.1 Experimental

Chemicals were purchased from Sigma-Aldrich and were used without further purification unless otherwise noted. Dialyses were performed using Spectra/Por regenerated cellulose membranes with either a 12000-14000 g/mol (Spectra/Por) or 3500 g/mol molecular weight cutoff (MWCO) cassettes. UV-visible absorption spectroscopy was performed on a Varian Cary 300 Bio UV-Visible Spectrophotometer. Extinction coefficients (ε) of compounds were obtained from calibration curves based on the measurement of UV-visible absorbance versus concentration in $CHCl_3$/MeOH (3/2). Dynamic light scattering (DLS) data were obtained using a Zetasizer Nano ZS instrument from Malvern Instruments. Compounds **1-9** were prepared as previously reported.[27,34,51] Spectral data agreed with those previously reported.

4.2 General Procedure for the Preparation of PEO-PBD Vesicles

Commercial block copolymer (4 equiv.) and azide-terminated polymer **7** (1 equiv.) were dissolved in CH_2Cl_2. The solvent was removed under a stream of nitrogen to produce a thin film. Deionized (DI) water (1mL/10mg of polymer) was added and the solution was stirred for 0.5 hours at 45 °C. The solution was then sonicated for 0.5 hours and finally stirred for 24 hours at 45 °C. The vesicles were extruded 2 times through each of 1000 nm, 400 nm, 200 nm and 100 nm polycarbonate membranes at 45 °C using a pressure driven Lipex Thermobarrel Extruder (1.5mL capacity, Northern Lipids) unless otherwise noted.

4.3 General Procedure for the Preparation of PEO-PCL Vesicles

The block copolymer **8** (4 equiv.) and **9** (1 equiv.) was dissolved in tetrahydrofuran (THF) (0.5 mL). DI water (2 mL) was added dropwise over 10 min with vigorous stirring. After the addition was complete, the resulting nanoassembly suspension was stirred for 10 min. and then

dialyzed against 2 L of DI water, using a 12,000–14,000 MWCO dialysis membrane, changing the dialysate approximately every 12 hours for 36 hours to remove THF.

4.4 General Procedure for Surface Functionalization of Vesicles

Vesicles were prepared as described above. To the assemblies were added $CuCl_2 \cdot 2H_2O$ (0.40 equiv. relative to azide terminated polymer), sodium ascorbate (4.0 equiv. relative to azide terminated polymer), and dendron in sequence and the reaction mixture was stirred at room temperature for 18 hours and then dialyzed against distilled water for 24 hours using a 12000-14000 MWCO dialysis membrane.

4.5 Quantification of Surface Dendritic Groups

Following dialysis of the dendron functionalized vesicles prepared as described above, the samples were lyophilized in order to remove water and were then taken up in 2 mL of $CHCl_3$/methanol 3/2. The solutions were centrifuged at 4500 rpm for 4 hours to remove any insoluble material. Finally, the absorbance was measured at 563 nm. The degree of functionalization was calculated using the measured ε for the dye-labeled dendrons **4** or **5**.

4.6 Encapsulation and Release of Small Molecules from Vesicles

Functionalized vesicles were prepared as described above, except rhodamine B (64mg) was dissolved in the water used for vesicle formation. In addition, the vesicle solution was extruded twice through only a 1000 nm polycarbonate membrane. After functionalization, different vesicle solutions were diluted to a concentration of 1 mg/mL of polymer, and dialysis was performed using a Slide-a-lyzer dialysis cassette with a MWCO of 3500 g/mol. A control dialysis containing rhodamine B in the same concentration within the dialysis cassette was

performed at the same time as the vesicle solution. When the dye had left the cassette in the control group, the release experiment was started (time = 0). The water was replaced with 0.1 M phosphate buffer water containing 0.01 M sodium azide at 37 °C. Every hour, 1 mL of the buffer from outside of the cassette was taken and the volume was topped up to maintain a continuous volume of 2 L. After 44 hours, the individual vesicle solutions were mixed with THF to disrupt the vesicles and release the free dye. The THF was removed under reduced pressure and the aqueous solution was returned to the dialysis cassette and allowed to stir for 24 hours. 1 mL of water from outside was taken as a 100% release standard for each trial. The fluorescence intensity of each sample was measured and compared to the 100% release sample to obtain the percent release at a given time point.

4.7 Encapsulation and Release of Protein from Vesicles

Functionalized vesicles were prepared as described above except rhodamine B labeled BSA (30mg) was dissolved in the water used for vesicle formation. In addition, the vesicle solution was extruded twice only through a 1000 nm polycarbonate membrane. After functionalization, different vesicle solutions were diluted to a polymer concentration of 1 mg/mL and dialysis was performed using a dialysis cassette with a MWCO of 300 kg/mol. A control experiment containing free rhodamine B labeled BSA in the same concentration was performed at the same time as the vesicle solutions. When the protein had left the cassette in the control group, the release experiment was started (time = 0). The water was replaced with 0.1 M phosphate buffer water containing 0.01 M sodium azide at 37°C. The vesicle solution was removed from the cassette and its fluorescence intensity was measured relative to a control of free rhodamine B labeled protein in solution. Each day the fluorescence intensity of the vesicle solutions in the

cassettes were taken relative to the free rhodamine B labeled protein solution, the volume of water was continuously maintained at 2L. After 15 days, the individual vesicle solutions were mixed with THF to disrupt the vesicles and release the free protein. The THF was removed under reduced pressure and the aqueous solution was returned to the dialysis cassette and allowed to stir for 24 hours. The fluorescence intensity of the aqueous samples were taken relative to the free rhodamine B labeled protein solution to determine the complete release value.

4.8 Procedure for MTT assay

HeLa cells were cultured in Dulbecco's Modified Eagle Medium (Invitrogen) supplemented with 10% fetal bovine serum (Invitrogen) at 37°C in an atmosphere containing 5% CO_2. Viability was measured using an MTT assay.[55] Cells were seeded into a 96-well plate (Nunclon TC treated) at a density of $4x10^3$ cells per well in growth medium with a final volume of 100 μL. The cells were allowed to adhere for 24 hours and then the medium was aspirated. To the cells, polymer vesicle samples were added at concentrations ranging from 1.0 mg/mL to 0.0078 mg/ml in 100 μL of growth medium. 8 replicates were performed for each concentration and to control cells only growth medium was added. The cells were incubated for 48 hours. The media was aspirated, then 100 μL of fresh media and 10 μL of MTT solution (5mg/mL) was added to each well and incubated for another 4 hours. Media was aspirated and the formazan product was solubilized by addition of 50 μL DMSO to each well. Absorbance of each well was measured at 540 nm using a plate reader (Tecan Safire).

4.9 Cell Uptake

HeLa cells were maintained at 37 °C and 5% CO_2 in Dulbecco's Modified Eagle Medium (Invitrogen) supplemented with 10% fetal bovine serum (Invitrogen). Sterilized microscope glass

cover slips (circular 25mm diameter) were placed in the wells of a 6-well plate and 5 x 10^5 cells were seeded onto each cover slip. The cells were allowed to adhere for 24 hours. The culture medium was then aspirated and replaced with fresh serum-free medium containing control or functionalized vesicles at a concentration of 0.25 mg/mL of polymer. The experiments were completed in triplicate. The cells were incubated at 37 °C for 1 hour. They were then washed three times with phosphate-buffered saline (PBS) then fixed with 4% paraformaldehyde solution for 10 min. The cells were washed again with PBS, and then treated with 2 mL of acetone at -20 °C for 5 minutes. The cells were washed again with PBS and stained with DAPI following the manufacturer's directions. The cells were washed again with PBS and then were placed face down onto microscope slides for confocal microscopy. Confocal images were obtained using a confocal laser scanning microscope (LSM 510, Carl Zeiss) using a 63x (N.A. ¼ 1.4) oil immersion objective and an excitation wavelength of 405 and 543 nm (He-Ne laser).

Part Five: References

(1) Wang, M.; Thanou, M. *Pharmacol. Res.* **2010**, *62*, 90.

(2) Bonduelle, C. V.; Gillies, E. R. *Pharmaceuticals* **2010**, *3*, 636.

(3) Choe, U. J.; Sun, V. Z.; Tan, J. K.; Kamei, D. T. *Top. Curr. Chem.* [Online Early Access]. DOI: 10.1007/128_2011_209. Published Online: 2011. (accessed Aug 2).

(4) Mariano, C.; Sasaki, H.; Brites, D.; Brito, M. A. *Eur. J. Cell Biol.* [Online Early Access]. DOI: 10.1016/j.ejcb.2011.06.005. Published Online: 2011. (accessed Aug 23).

(5) Chao, T. Y.; Raines, R. T. *Biochemistry* [Online Early Access]. DOI: 10.1021/bi2009079. Published Online: 2011. (accessed Aug 9).

(6) Sun, V. Z.; Li, Z.; Deming, T. J.; Kamei, D. T. *Biomacromolecules* **2011**, *12*, 10.

(7) Bretscher, M. S. *Sci. Am.* **1985**, *253*, 100.

(8) Monnard, P. A.; Deamer, D. W. *Anat. Rec.* **2002**, *268*, 196.

(9) Zhang, T.; Li, Y.; Mueller, A. *Chem. Phys. Lipids* [Online Early Access]. DOI: 10.1016/j.chemphyslip.2011.08.004. Published Online: 2011. (accessed Aug 19).

(10) Peptu, C.; Popa, M.; Antimisiaris, S. G. *J. Nanosci. Nanotechnol.* **2008**, *8*, 2249.

(11) Sagar, G. H.; Bellare, J. R. *J. Phys. Chem. B* **2009**, *113*, 13805.

(12) McNeil, S. E.; Vangala, A.; Bramwell, V. W.; Hanson, P. J.; Perrie, Y. *Curr. Drug Delivery* **2010**, *7*, 175.

(13) Maestrelli, F.; Capasso, G.; Gonzalez-Rodriguez, M. L.; Rabasco, A. M.; Ghelardini, C.; Mura, P. *J. Liposome Res.* **2009**, *19*, 253.

(14) Zaru, M.; Manca, M. L.; Fadda, A. M.; Antimisiaris, S. G. *Colloids Surf. B Biointerfaces* **2009**, *71*, 88.

(15) Photos, P. J.; Bacakova, L.; Discher, B.; Bates, F. S.; Discher, D. E. *J. Controlled Release* **2003**, *90*, 323.

(16) Lasic, D. D.; Papahadjopoulos, D. *Current Opinion in Solid State and Materials Science* **1996**, *1*, 392.

(17) Discher, D. E.; Ahmed, F. *Annu. Rev. Biomed. Eng.* **2006**, *8*, 323.

(18) Zhang, L.; Eisenberg, A. *Science* **1995**, *268*, 1728.

(19) Li, X. G.; Lu, Q. F.; Huang, M. R. *Small* **2008**, *4*, 1201.

(20) Yoshikawa, H. Y.; Rossetti, F. F.; Kaufmann, S.; Kaindl, T.; Madsen, J.; Engel, U.; Lewis, A. L.; Armes, S. P.; Tanaka, M. *J. Am. Chem. Soc.* **2011**, *133*, 1367.

(21) Li, X.; Mya, K. Y.; Ni, X.; He, C.; Leong, K. W.; Li, J. *J. Phys. Chem. B* **2006**, *110*, 5920.

(22) Discher, B. M.; Won, Y. Y.; Ege, D. S.; Lee, J. C.; Bates, F. S.; Discher, D. E.; Hammer, D. A. *Science* **1999**, *284*, 1143.

(23) Discher, D. E.; Eisenberg, A. *Science* **2002**, *297*, 967.

(24) Zhang, L. F.; Eisenberg, A. *J. Am. Chem. Soc.* **1996**, *118*, 3168.

(25) Mackiewicz, N.; Gravel, E.; Garofalakis, A.; Ogier, J.; John, J.; Dupont, D. M.; Gombert, K.; Tavitian, B.; Doris, E.; Duconge, F. *Small* [Online Early Access]. DOI: 10.1002/smll.201100212. Published Online: 2011. (accessed Aug 12).

(26) O'Reilly, R. K.; Hawker, C. J.; Wooley, K. L. *Chem. Soc. Rev.* **2006**, *35*, 1068.

(27) Nazemi, A.; Amos, R. C.; Bonduelle, C. V.; Gillies, E. R. *J. of Polym. Sci. A-Polym. Chem.* **2011**, *49*, 2546.

(28) Rijcken, C. J. F.; Soga, O.; Hennink, W. E.; van Nostrum, C. F. *J. Controlled Release* **2007**, *120*, 131.

(29) Simnick, A. J.; Amiram, M.; Liu, W.; Hanna, G.; Dewhirst, M. W.; Kontos, C. D.; Chilkoti, A. *J. Controlled Release* [Online Early Access]. DOI: 10.1016/j.jconrel.2011.06.044. Published Online: 2011. (accessed Jul 8).

(30) Du, J. Z.; O'Reilly, R. K. *Soft Matter* **2009**, *5*, 3544.

(31) Du, J. Z.; Armes, S. P. *J. Am. Chem. Soc.* **2005**, *127*, 12800.

(32) Cerritelli, S.; Velluto, D.; Hubbell, J. A. *Biomacromolecules* **2007**, *8*, 1966.

(33) Boerakker, M. J.; Botterhuis, N. E.; Bomans, P. H. H.; Frederik, P. M.; Meijer, E. M.; Nolte, R. J. M.; Sommerdijk, N. *Chem. Eur. J.* **2006**, *12*, 6071.

(34) Li, B.; Martin, A. L.; Gillies, E. R. *Chem. Commun.* **2007**, 5217.

(35) Borchert, U.; Lipprandt, U.; Bilang, M.; Kimpfler, A.; Rank, A.; Peschka-Suss, R.; Schubert, R.; Lindner, P.; Forster, S. *Langmuir* **2006**, *22*, 5843.

(36) Shum, H. C.; Santanach-Carreras, E.; Kim, J. W.; Ehrlicher, A.; Bibette, J.; Weitz, D. A. *J. Am. Chem. Soc.* **2011**, *133*, 4420.

(37) Kim, S. H.; Shum, H. C.; Kim, J. W.; Cho, J. C.; Weitz, D. A. *J. Am. Chem. Soc.* [Online Early Access]. DOI: 10.1021/ja205687k. Published Online: 2011. (accessed Aug 12).

(38) Christian, D. A.; Cai, S.; Bowen, D. M.; Kim, Y.; Pajerowski, J. D.; Discher, D. E. *Eur. J. Pharm. Biopharm.* **2009**, *71*, 463.

(39) Kim, Y.; Tewari, M.; Pajerowski, J. D.; Cai, S.; Sen, S.; Williams, J. H.; Sirsi, S. R.; Lutz, G. J.; Discher, D. E. *J. Control. Release* **2009**, *134*, 132.

(40) Mueller, W.; Koynov, K.; Fischer, K.; Hartmann, S.; Pierrat, S.; Basche, T.; Maskos, M. *Abstr. Pap. Am. Chem. Soc.* **2009**, *237*.

(41) Ahmed, F.; Pakunlu, R. I.; Srinivas, G.; Brannan, A.; Bates, F.; Klein, M. L.; Minko, T.; Discher, D. E. *Mol. Pharm.* **2006**, *3*, 340.

(42) Holowka, E. P.; Sun, V. Z.; Kamei, D. T.; Deming, T. J. *Nat. Mater.* **2007**, *6*, 52.

(43) Biswas, S.; Dodwadkar, N. S.; Sawant, R. R.; Torchilin, V. *Bioconjugate Chem.* [Online Early Access]. DOI: 10.1021/bc2002133. Published Online: 2011. (accessed Aug 29).

(44) Opsteen, J. A.; Brinkhuis, R. P.; Teeuwen, R. L. M.; Lowik, D. W. P. M.; van Hest, J. C. M. *Chem. Commun.* **2007**, 3136.

(45) Lin, J. J.; Silas, J. A.; Bermudez, H.; Milam, V. T.; Bates, F. S.; Hammer, D. A. *Langmuir* **2004**, *20*, 5493.

(46) Lin, J. J.; Ghoroghchian, P.; Zhang, Y.; Hammer, D. A. *Langmuir* **2006**, *22*, 3975.

(47) Broz, P.; Benito, S. M.; Saw, C.; Burger, P.; Heider, H.; Pfisterer, M.; Marsch, S.; Meier, W.; Hunziker, P. *J. Controlled Release* **2005**, *102*, 475.

(48) Martin, A. L.; Li, B.; Gillies, E. R. *J. Am. Chem. Soc.* **2009**, *131*, 734.

(49) Saalik, P.; Elmquist, A.; Hansen, M.; Padari, K.; Saar, K.; Viht, K.; Langel, U.; Pooga, M. *Bioconjugate Chem.* **2004**, *15*, 1246.

(50) Schwarze, S. R.; Hruska, K. A.; Dowdy, S. F. *Trends Cell Biol.* **2000**, *10*, 290.

(51) Martin, A. L.; Bernas, L. M.; Rutt, B. K.; Foster, P. J.; Gillies, E. R. *Bioconjugate Chem.* **2008**, *19*, 2375.

(52) Mintzer, M. A.; Merkel, O. M.; Kissel, T.; Simanek, E. E. *New J. Chem.* **2009**, *33*, 1918.

(53) Tziveleka, L. A.; Psarra, A. M.; Tsiourvas, D.; Paleos, C. M. *J. Controlled Release* **2007**, *117*, 137.

(54) Doherty, A. T.; Hayes, J.; Fellows, M.; Kirk, S.; O'Donovan, M. *Mutat. Res.* [Online Early Access]. DOI: 10.1016/j.mrgentox.2011.08.002. Published Online: 2011. (accessed Aug 26).

(55) Freshney, I. *Cell Biol. Toxicol.* **2001**, *17*, 213.